Protein Cell 2017, 8(6):401–438
DOI 10.1007/s13238-017-0372-z

Protein & Cell

RESOURCE

Structure-based assessment of disease-related mutations in human voltage-gated sodium channels

Weiyun Huang[1,2,3], Minhao Liu[2], S. Frank Yan[4]✉, Nieng Yan[1,2,3]✉

[1] State Key Laboratory of Membrane Biology, School of Life Sciences and School of Medicine, Tsinghua University, Beijing 100084, China
[2] Beijing Advanced Innovation Center for Structural Biology, School of Life Sciences and School of Medicine, Tsinghua University, Beijing 100084, China
[3] Tsinghua-Peking Joint Center for Life Sciences, School of Life Sciences and School of Medicine, Tsinghua University, Beijing 100084, China
[4] Molecular Design and Chemical Biology, Roche Pharma Research and Early Development, Roche Innovation Center Shanghai, Shanghai 201203, China
✉ Correspondence: frank.yan@outlook.com (S. F. Yan), nyan@tsinghua.edu.cn (N. Yan)
Received November 18, 2016 Accepted January 9, 2017

ABSTRACT

Voltage-gated sodium (Na_v) channels are essential for the rapid upstroke of action potentials and the propagation of electrical signals in nerves and muscles. Defects of Na_v channels are associated with a variety of channelopathies. More than 1000 disease-related mutations have been identified in Na_v channels, with $Na_v1.1$ and $Na_v1.5$ each harboring more than 400 mutations. Na_v channels represent major targets for a wide array of neurotoxins and drugs. Atomic structures of Na_v channels are required to understand their function and disease mechanisms. The recently determined atomic structure of the rabbit voltage-gated calcium (Ca_v) channel $Ca_v1.1$ provides a template for homology-based structural modeling of the evolutionarily related Na_v channels. In this Resource article, we summarized all the reported disease-related mutations in human Na_v channels, generated a homologous model of human $Na_v1.7$, and structurally mapped disease-associated mutations. Before the determination of structures of human Na_v channels, the analysis presented here serves as the base framework for mechanistic investigation of Na_v channelopathies and for potential structure-based drug discovery.

KEYWORDS Na_v channels, channelopathy, $Na_v1.7$, structure modeling, pain

INTRODUCTION

Voltage-gated sodium (Na_v) channels are essential for the rapid depolarization phase of action potential and play a key role in the electrical signaling in most excitable cells. Structurally, Na_v channels are composed of one α subunit and one or more β subunits. The α subunit contains two functionally distinct structural entities, namely, the voltage-sensing domains (VSDs) and the ion-conducting pore domain (Catterall, 2012b, 2014). The β subunits, which bind to α subunit covalently or non-covalently, modulate membrane trafficking, voltage dependence, and channel gating kinetics (Catterall, 2012b, 2014). In mammals, Na_v channels have nine known α members distributed in different excitable tissues. Specifically, $Na_v1.1$, $Na_v1.2$, $Na_v1.3$, and $Na_v1.6$ are the primary sodium channels in central nervous system (CNS), $Na_v1.4$ is primarily expressed in skeletal muscle, $Na_v1.5$ is mainly expressed in heart, and $Na_v1.7$, $Na_v1.8$, and $Na_v1.9$ are mainly distributed in peripheral nervous system (Plummer and Meisler, 1999; Goldin, 2001; Catterall et al., 2005).

All α subunits share nearly identical structure topology—a canonical voltage-gated ion channel fold with four homologous repeats, each containing six transmembrane segments S1–S6. Specifically, S5–S6 segments form the pore domain that conducts selective sodium filtering, while S1–S4 segments constitute the voltage-sensing domain that controls voltage-dependent gating (Catterall, 2000). The voltage sensors in the VSDs are featured by a number of positively charged amino acids (arginine or lysine) located at every

Table 1. Structural mapping of disease-related mutations identified in human $Na_v1.7$

Related proteins	Mutations	Diseases	Structural position	Map on $hNa_v1.7$
$hNa_v1.7$	Q10R	IEM	N-terminus	Q10
$hNa_v1.7$	I62V	FEB	N-terminus	I62
$hNa_v1.7$	I136V	IEM	DI S1	I136
$hNa_v1.7$	P149Q	FEB	DI S1-S2	P149
$hNa_v1.7$	R185H	PEPD	DI S3	R185
$hNa_v1.7$	R185H	SFN	DI S3	R185
$hNa_v1.7$	S211P	IEM	DI S3-S4	S211
$hNa_v1.7$	F216S	IEM	DI S4	F216
$hNa_v1.7$	I228M	DS	DI S4	I228
$hNa_v1.7$	I228M	SFN	DI S4	I228
$hNa_v1.7$	I234T	IEM	DI S5	I234
$hNa_v1.7$	S241T	IEM	DI S5	S241
$hNa_v1.7$	L245V	IEM	DI S5	L245
$hNa_v1.7$	N395K	IEM	DI S6	N395
$hNa_v1.7$	V400M	IEM	DI S6	V400
$hNa_v1.7$	E406K	IEM	DI S6	E406
$hNa_v1.7$	S490N	FEB	DI - DII	S490
$hNa_v1.7$	E519K	DS	DI - DII	E519
$hNa_v1.7$	P610T	IEM	DI - DII	P610
$hNa_v1.7$	G616R	IEM	DI - DII	G616
$hNa_v1.7$	D623N	SFN	DI - DII	D623
$hNa_v1.7$	N641Y	FEB	DI - DII	N641
$hNa_v1.7$	K666R	FEB	DI - DII	K666
$hNa_v1.7$	K666R	DS	DI - DII	K666
$hNa_v1.7$	I695M	DS	DI - DII	I695
$hNa_v1.7$	C710Y	DS	DI - DII	C710
$hNa_v1.7$	I731K	SFN	DI - DII	I731
$hNa_v1.7$	I750V	SFN	DII S1	I750
$hNa_v1.7$	I750V	DS	DII S1	I750
$hNa_v1.7$	I750V	FEB	DII S1	I750
$hNa_v1.7$	L834R	IEM	DII S4	L834
$hNa_v1.7$	I859T	IEM	DII S5	I859
$hNa_v1.7$	G867D	IEM	DII S5	G867
$hNa_v1.7$	L869F	IEM	DII S5	L869
$hNa_v1.7$	L869H	IEM	DII S5	L869
$hNa_v1.7$	A874P	IEM	DII S5	A874
$hNa_v1.7$	V883G	IEM	DII S5	V883
$hNa_v1.7$	Q886E	IEM	DII S5	Q886
$hNa_v1.7$	R907Q	CIP	DII S5-S6	R907
$hNa_v1.7$	M943L	SFN	DII S5-S6	M943
$hNa_v1.7$	V1002L	SFN	DII - DIII	V1002
$hNa_v1.7$	R1007C	PEPD	DII - DIII	R1007
$hNa_v1.7$	L1134F	DS	DII - DIII	L1134

Table 1 continued

Related proteins	Mutations	Diseases	Structural position	Map on $hNa_v1.7$
$hNa_v1.7$	E1171Q	DS	DII - DIII	E1171
$hNa_v1.7$	A1247E	CIP	DIII S2	A1247
$hNa_v1.7$	L1278V	DS	DIII S3-S4	L1278
$hNa_v1.7$	V1309D	PEPD	DIII S4-S5	V1309
$hNa_v1.7$	V1309F	PEPD	DIII S4-S5	V1309
$hNa_v1.7$	V1310F	PEPD	DIII S4-S5	V1310
$hNa_v1.7$	P1319L	IEM	DIII S4-S5	P1319
$hNa_v1.7$	F1460V	IEM	DIII S6	F1460
$hNa_v1.7$	I1472T	PEPD	DIII - DIV	I1472
$hNa_v1.7$	F1473V	PEPD	DIII - DIV	F1473
$hNa_v1.7$	T1475I	PEPD	DIII - DIV	T1475
$hNa_v1.7$	M1543I	SFN	DIV S2	M1543
$hNa_v1.7$	G1618R	PEPD	DIV S4	G1618
$hNa_v1.7$	L1623P	PEPD	DIV S4	L1623
$hNa_v1.7$	M1638K	PEPD	DIV S5	M1638
$hNa_v1.7$	A1643E	PEPD	DIV S5	A1643
$hNa_v1.7$	A1643E	IEM	DIV S5	A1643
$hNa_v1.7$	A1643G	IEM	DIV S5	A1643
$hNa_v1.7$	A1643T	IEM	DIV S5	A1643
$hNa_v1.7$	W1786R	CIP	C-terminus	W1786

IEM: Primary erythermalgia; PEPD: Paroxysmal extreme pain disorder; CIP: Indifference to pain, congenital, autosomal recessive; DS: Dravet syndrome; SFN: Small fiber neuropathy; FEB: Febrile seizures.

third position in the S4 segment. Upon membrane depolarization, movements of these charged residues in the S4 segment are coupled to the opening of the pore domain and the subsequent influx of sodium ions across cell membrane. The pore domain is structurally organized with a four-fold pseudo-symmetry. The pore (P) loops, which are supported by the P1 helix (corresponding to the P helix in potassium channel) and P2 helix between S5 and S6 segments in each repeat, constitute the selectivity filter (SF) (Corry and Thomas, 2012). Four amino acid residues (aspartate, glutamate, lysine, and alanine, DEKA, in repeats I, II, III, and IV, respectively) in the P loops are crucial for sodium selectivity. Mutating these residues to glutamates confers calcium selectivity, suggesting that the side chains of these amino acids are likely to interact directly with the sodium ions to determine ion selectivity (Heinemann et al., 1992; Sun et al., 1997).

Na_v channels inactivate rapidly. A cluster of hydrophobic amino acids (isoleucine, phenylalanine, methionine, and threonine), namely the IFMT motif, located in the cytosolic regions of domain III and domain IV, are required for rapid inactivation. This is demonstrated by the fact that rapid inactivation could be achieved by titrating small peptides containing the IFMT motif (Vassilev et al., 1988; West et al., 1992).

Sodium channelopathies are a group of diseases caused by defective Na_v channels, either, in most cases, of congenital nature or acquired nature (Tables 1, 2, 3, 4, 5, 6, 7, 8, 9, 10) (George, 2005; Catterall, 2012a; Kim, 2014). For example, $Na_v1.1$ is primarily expressed in the soma of neuronal cells in the CNS, and mutations of $Na_v1.1$ cause GEFS+2 (generalized epilepsy with febrile seizures plus 2) (Catterall et al., 2010). Moreover, mutations of $Na_v1.1$ are also the main causes of EIEE6 (epileptic encephalopathy, early infantile, 6) and ICEGTC (intractable childhood epilepsy with generalized tonic-clonic seizures) (Escayg and Goldin, 2010). $Na_v1.5$ is the major sodium channel expressed in heart. $Na_v1.5$ mutations may lead to various cardiac diseases such as LQT3 (long QT syndrome 3), BRGDA1 (Brugada syndrome 1), and SSS1 (sick sinus syndrome 1) (Olson et al., 2005; Song and Shou, 2012; Veerman et al., 2015). $Na_v1.7$ is preferentially expressed in the sympathetic neurons, olfactory epithelium, and dorsal root ganglion sensory neurons, and plays a cardinal role in pain

Table 2. Structural mapping of disease-related mutations identified in human $Na_v1.1$

Related proteins	Mutations	Diseases	Structural position	Map on $hNa_v1.7$
$hNa_v1.1$	R27T	GEFS+2	N-terminus	Q25
$hNa_v1.1$	S74P	GEFS+2	N-terminus	S72
$hNa_v1.1$	D188V	GEFS+2	DI S3	D186
$hNa_v1.1$	F218L	GEFS+2	DI S4	F216
$hNa_v1.1$	T254I	GEFS+2	DI S5	T252
$hNa_v1.1$	S291G	GEFS+2	DI S5-S6	S279
$hNa_v1.1$	R377Q	GEFS+2	DI S5-S6	R356
$hNa_v1.1$	Y388H	GEFS+2	DI S5-S6	Y367
$hNa_v1.1$	Y790C	GEFS+2	DII S1-S2	H766
$hNa_v1.1$	R859C	GEFS+2	DII S4	R835
$hNa_v1.1$	R859H	GEFS+2	DII S4	R835
$hNa_v1.1$	T875M	GEFS+2	DII S4-S5	T851
$hNa_v1.1$	I899T	GEFS+2	DII S5	I875
$hNa_v1.1$	N935H	GEFS+2	DII S5-S6	N911
$hNa_v1.1$	R946H	GEFS+2	DII S5-S6	R922
$hNa_v1.1$	M960T	GEFS+2	DII S5-S6	M936
$hNa_v1.1$	M973V	GEFS+2	DII S6	M949
$hNa_v1.1$	M976I	GEFS+2	DII S6	M952
$hNa_v1.1$	I978M	GEFS+2	DII S6	I954
$hNa_v1.1$	W1204R	GEFS+2	DII - DIII	W1178
$hNa_v1.1$	W1204S	GEFS+2	DII - DIII	W1178
$hNa_v1.1$	L1230F	GEFS+2	DIII S1	L1204
$hNa_v1.1$	K1249N	GEFS+2	DIII S2	K1223
$hNa_v1.1$	T1250M	GEFS+2	DIII S2	I1224
$hNa_v1.1$	K1270T	GEFS+2	DIII S2	K1244
$hNa_v1.1$	L1309F	GEFS+2	DIII S3-S4	L1283
$hNa_v1.1$	V1353L	GEFS+2	DIII S5	V1327
$hNa_v1.1$	V1366I	GEFS+2	DIII S5	V1340
$hNa_v1.1$	N1414D	GEFS+2	DIII S5-S6	N1388
$hNa_v1.1$	V1428A	GEFS+2	DIII S5-S6	V1402
$hNa_v1.1$	R1596H	GEFS+2	DIV S2-S3	R1570
$hNa_v1.1$	R1648H	GEFS+2	DIV S4	R1622
$hNa_v1.1$	I1656M	GEFS+2	DIV S5	I1630
$hNa_v1.1$	R1657C	GEFS+2	DIV S5	R1631
$hNa_v1.1$	A1685V	GEFS+2	DIV S5	A1659
$hNa_v1.1$	F1687S	GEFS+2	DIV S5	F1661
$hNa_v1.1$	P1739L	GEFS+2	DIV S5-S6	P1713
$hNa_v1.1$	D1742G	GEFS+2	DIV S5-S6	D1716
$hNa_v1.1$	F1765L	GEFS+2	DIV S6	Y1739
$hNa_v1.1$	E1795K	GEFS+2	C-terminus	E1769
$hNa_v1.1$	M1852T	GEFS+2	C-terminus	M1826
$hNa_v1.1$	V1857L	GEFS+2	C-terminus	V1831
$hNa_v1.1$	D1866Y	GEFS+2	C-terminus	D1840

Table 2 continued

Related proteins	Mutations	Diseases	Structural position	Map on $hNa_v1.7$
$hNa_v1.1$	I1867T	GEFS+2	C-terminus	I1841
$hNa_v1.1$	G58V	EIEE6	N-terminus	G56
$hNa_v1.1$	L61F	EIEE6	N-terminus	L59
$hNa_v1.1$	F63L	EIEE6	N-terminus	F61
$hNa_v1.1$	I68T	EIEE6	N-terminus	I66
$hNa_v1.1$	E78D	EIEE6	N-terminus	E76
$hNa_v1.1$	D79H	EIEE6	N-terminus	D77
$hNa_v1.1$	D79N	EIEE6	N-terminus	D77
$hNa_v1.1$	Y84C	EIEE6	N-terminus	Y82
$hNa_v1.1$	F90S	EIEE6	N-terminus	F88
$hNa_v1.1$	I91T	EIEE6	N-terminus	I89
$hNa_v1.1$	A98P	EIEE6	N-terminus	T96
$hNa_v1.1$	R101Q	EIEE6	N-terminus	R99
$hNa_v1.1$	R101W	EIEE6	N-terminus	R99
$hNa_v1.1$	S103G	EIEE6	N-terminus	N101
$hNa_v1.1$	T105I	EIEE6	N-terminus	T103
$hNa_v1.1$	L108R	EIEE6	N-terminus	L106
$hNa_v1.1$	T112I	EIEE6	N-terminus	S110
$hNa_v1.1$	R118S	EIEE6	N-terminus	R116
$hNa_v1.1$	I124N	EIEE6	N-terminus	I122
$hNa_v1.1$	H127D	EIEE6	N-terminus	H125
$hNa_v1.1$	T162P	EIEE6	DI S2	T160
$hNa_v1.1$	I171K	EIEE6	DI S2	V169
$hNa_v1.1$	I171R	EIEE6	DI S2	V169
$hNa_v1.1$	A175T	EIEE6	DI S2-23	A173
$hNa_v1.1$	A175V	EIEE6	DI S2-S3	A173
$hNa_v1.1$	G177E	EIEE6	DI S2-S3	G175
$hNa_v1.1$	C179R	EIEE6	DI S2-S3	C177
$hNa_v1.1$	W190R	EIEE6	DI S3	W188
$hNa_v1.1$	N191K	EIEE6	DI S3	N189
$hNa_v1.1$	N191Y	EIEE6	DI S3	N189
$hNa_v1.1$	D194G	EIEE6	DI S3	D192
$hNa_v1.1$	D194N	EIEE6	DI S3	D192
$hNa_v1.1$	T199R	EIEE6	DI S3	V197
$hNa_v1.1$	T217K	EIEE6	DI S3-S4	T215
$hNa_v1.1$	A223E	EIEE6	DI S4	A221
$hNa_v1.1$	T226M	EIEE6	DI S4	T224
$hNa_v1.1$	T226R	EIEE6	DI S4	T224
$hNa_v1.1$	I227S	EIEE6	DI S4	I225
$hNa_v1.1$	I227T	EIEE6	DI S4	I225
$hNa_v1.1$	G232S	EIEE6	DI S4-S5	G230
$hNa_v1.1$	L233R	EIEE6	DI S5	L231

Table 2 continued

Related proteins	Mutations	Diseases	Structural position	Map on $hNa_v1.7$
$hNa_v1.1$	A239T	EIEE6	DI S5	A237
$hNa_v1.1$	A239V	EIEE6	DI S5	A237
$hNa_v1.1$	S243Y	EIEE6	DI S5	S241
$hNa_v1.1$	I252N	EIEE6	DI S5	I250
$hNa_v1.1$	S259R	EIEE6	DI S5	S257
$hNa_v1.1$	G265W	EIEE6	DI S5	G263
$hNa_v1.1$	C277R	EIEE6	DI S5-S6	C275
$hNa_v1.1$	W280C	EIEE6	DI S5-S6	N278
$hNa_v1.1$	W280R	EIEE6	DI S5-S6	N278
$hNa_v1.1$	P281A	EIEE6	DI S5-S6	S279
$hNa_v1.1$	P281L	EIEE6	DI S5-S6	S279
$hNa_v1.1$	P281S	EIEE6	DI S5-S6	S279
$hNa_v1.1$	E289V	EIEE6	DI S5-S6	E287
$hNa_v1.1$	T297I	EIEE6	DI S5-S6	–
$hNa_v1.1$	R322I	EIEE6	DI S5-S6	R301
$hNa_v1.1$	S340F	EIEE6	DI S5-S6	T319
$hNa_v1.1$	A342V	EIEE6	DI S5-S6	S321
$hNa_v1.1$	G343D	EIEE6	DI S5-S6	G322
$hNa_v1.1$	C345R	EIEE6	DI S5-S6	C324
$hNa_v1.1$	C351W	EIEE6	DI S5-S6	C330
$hNa_v1.1$	G355D	EIEE6	DI S5-S6	G334
$hNa_v1.1$	R356G	EIEE6	DI S5-S6	R335
$hNa_v1.1$	N357I	EIEE6	DI S5-S6	N336
$hNa_v1.1$	P358T	EIEE6	DI S5-S6	P357
$hNa_v1.1$	N359S	EIEE6	DI S5-S6	D338
$hNa_v1.1$	T363P	EIEE6	DI S5-S6	T342
$hNa_v1.1$	T363R	EIEE6	DI S5-S6	T342
$hNa_v1.1$	D366E	EIEE6	DI S5-S6	D345
$hNa_v1.1$	L378Q	EIEE6	DI S5-S6	L357
$hNa_v1.1$	M379R	EIEE6	DI S5-S6	M358
$hNa_v1.1$	F383L	EIEE6	DI S5-S6	Y362
$hNa_v1.1$	W384R	EIEE6	DI S5-S6	M363
$hNa_v1.1$	R393C	EIEE6	DI S5-S6	R372
$hNa_v1.1$	R393H	EIEE6	DI S5-S6	R372
$hNa_v1.1$	R393S	EIEE6	DI S5-S6	R372
$hNa_v1.1$	M400V	EIEE6	DI S5-S6	M379
$hNa_v1.1$	F403L	EIEE6	DI S6	F383
$hNa_v1.1$	F403V	EIEE6	DI S6	F382
$hNa_v1.1$	V406F	EIEE6	DI S6	V385
$hNa_v1.1$	L409W	EIEE6	DI S6	L388
$hNa_v1.1$	Y413N	EIEE6	DI S6	Y392
$hNa_v1.1$	Y426C	EIEE6	DI S6	Y405

Table 2 continued

Related proteins	Mutations	Diseases	Structural position	Map on $hNa_v1.7$
$hNa_v1.1$	Y426N	EIEE6	DI S6	Y405
$hNa_v1.1$	S525F	EIEE6	DI - DII	S505
$hNa_v1.1$	S626G	EIEE6	DI - DII	S606
$hNa_v1.1$	D674G	EIEE6	DI - DII	D651
$hNa_v1.1$	N762D	EIEE6	DI - DII	Y738
$hNa_v1.1$	L783P	EIEE6	DII S1	L759
$hNa_v1.1$	M785T	EIEE6	DII S1-S2	M761
$hNa_v1.1$	T812I	EIEE6	DII S2	A788
$hNa_v1.1$	T812R	EIEE6	DII S2	A788
$hNa_v1.1$	L842R	EIEE6	DII S3	L818
$hNa_v1.1$	S843R	EIEE6	DII S3	S819
$hNa_v1.1$	E846K	EIEE6	DII S3	E822
$hNa_v1.1$	R859C	EIEE6	DII S4	R835
$hNa_v1.1$	R862Q	EIEE6	DII S4	R838
$hNa_v1.1$	R865G	EIEE6	DII S4	R841
$hNa_v1.1$	T875K	EIEE6	DII S4-S5	T851
$hNa_v1.1$	T875M	EIEE6	DII S4-S5	T851
$hNa_v1.1$	L876I	EIEE6	DII S5	L852
$hNa_v1.1$	L890P	EIEE6	DII S5	L866
$hNa_v1.1$	V896F	EIEE6	DII S5	V872
$hNa_v1.1$	V896L	EIEE6	DII S5	V872
$hNa_v1.1$	F902C	EIEE6	DII S5	F878
$hNa_v1.1$	C927F	EIEE6	DII S5-S6	C903
$hNa_v1.1$	R931C	EIEE6	DII S5-S6	R907
$hNa_v1.1$	W932C	EIEE6	DII S5-S6	W908
$hNa_v1.1$	H933P	EIEE6	DII S5-S6	H909
$hNa_v1.1$	M934I	EIEE6	DII S5-S6	M910
$hNa_v1.1$	H939P	EIEE6	DII S5-S6	H915
$hNa_v1.1$	H939Q	EIEE6	DII S5-S6	H915
$hNa_v1.1$	H939Y	EIEE6	DII S5-S6	H915
$hNa_v1.1$	S940F	EIEE6	DII S5-S6	S916
$hNa_v1.1$	L942P	EIEE6	DII S5-S6	L918
$hNa_v1.1$	I943N	EIEE6	DII S5-S6	I919
$hNa_v1.1$	V944A	EIEE6	DII S5-S6	V920
$hNa_v1.1$	V944E	EIEE6	DII S5-S6	V920
$hNa_v1.1$	F945L	EIEE6	DII S5-S6	F921
$hNa_v1.1$	R946C	EIEE6	DII S5-S6	R922
$hNa_v1.1$	R946H	EIEE6	DII S5-S6	R922
$hNa_v1.1$	R946S	EIEE6	DII S5-S6	R922
$hNa_v1.1$	C949S	EIEE6	DII S5-S6	C925
$hNa_v1.1$	C949Y	EIEE6	DII S5-S6	C925
$hNa_v1.1$	G950E	EIEE6	DII S5-S6	G926

Table 2 continued

Related proteins	Mutations	Diseases	Structural position	Map on $hNa_v1.7$
$hNa_v1.1$	G950R	EIEE6	DII S5-S6	G926
$hNa_v1.1$	W952G	EIEE6	DII S5-S6	W928
$hNa_v1.1$	E954K	EIEE6	DII S5-S6	E930
$hNa_v1.1$	M956K	EIEE6	DII S5-S6	M932
$hNa_v1.1$	W957L	EIEE6	DII S5-S6	W933
$hNa_v1.1$	C959R	EIEE6	DII S5-S6	C935
$hNa_v1.1$	M960V	EIEE6	DII S5-S6	M936
$hNa_v1.1$	M973K	EIEE6	DII S6	M949
$hNa_v1.1$	M976I	EIEE6	DII S6	M952
$hNa_v1.1$	G979V	EIEE6	DII S6	G955
$hNa_v1.1$	N985I	EIEE6	DII S6	N961
$hNa_v1.1$	L986F	EIEE6	DII S6	L962
$hNa_v1.1$	L986P	EIEE6	DII S6	L962
$hNa_v1.1$	F987L	EIEE6	DII S6	F963
$hNa_v1.1$	S993R	EIEE6	DII - DIII	S969
$hNa_v1.1$	D998G	EIEE6	DII - DIII	D974
$hNa_v1.1$	E1068K	EIEE6	DII - DIII	E1045
$hNa_v1.1$	L1207P	EIEE6	DII - DIII	I1181
$hNa_v1.1$	R1208K	EIEE6	DII - DIII	R1182
$hNa_v1.1$	T1210K	EIEE6	DII - DIII	T1184
$hNa_v1.1$	E1221K	EIEE6	DIII S1	E1195
$hNa_v1.1$	L1230F	EIEE6	DIII S1	L1204
$hNa_v1.1$	S1231R	EIEE6	DIII S1	S1205
$hNa_v1.1$	S1231T	EIEE6	DIII S1	S1205
$hNa_v1.1$	G1233R	EIEE6	DIII S1	G1207
$hNa_v1.1$	E1238D	EIEE6	DIII S1-S2	E1212
$hNa_v1.1$	D1239G	EIEE6	DIII S1-S2	D1213
$hNa_v1.1$	D1239Y	EIEE6	DIII S1-S2	D1213
$hNa_v1.1$	R1245Q	EIEE6	DIII S1-S2	K1219
$hNa_v1.1$	A1255D	EIEE6	DIII S2	A1229
$hNa_v1.1$	T1260P	EIEE6	DIII S2	T1234
$hNa_v1.1$	F1263L	EIEE6	DIII S2	F1237
$hNa_v1.1$	L1265P	EIEE6	DIII S2	L1239
$hNa_v1.1$	E1266A	EIEE6	DIII S2	E1240
$hNa_v1.1$	G1275V	EIEE6	DIII S2-S3	G1249
$hNa_v1.1$	W1284S	EIEE6	DIII S3	W1258
$hNa_v1.1$	L1287P	EIEE6	DIII S3	L1261
$hNa_v1.1$	D1288N	EIEE6	DIII S3	D1262
$hNa_v1.1$	R1316G	EIEE6	DIII S4	R1290
$hNa_v1.1$	R1316S	EIEE6	DIII S4	R1290
$hNa_v1.1$	A1320V	EIEE6	DIII S4	A1294
$hNa_v1.1$	A1326P	EIEE6	DIII S4	A1300

Table 2 continued

Related proteins	Mutations	Diseases	Structural position	Map on $hNa_v1.7$
$hNa_v1.1$	S1328P	EIEE6	DIII S4-S5	S1302
$hNa_v1.1$	V1335M	EIEE6	DIII S4-S5	V1309
$hNa_v1.1$	A1339V	EIEE6	DIII S4-S5	A1313
$hNa_v1.1$	I1344M	EIEE6	DIII S4-S5	I1318
$hNa_v1.1$	V1350G	EIEE6	DIII S5	V1324
$hNa_v1.1$	L1355P	EIEE6	DIII S5	L1329
$hNa_v1.1$	W1358R	EIEE6	DIII S5	W1332
$hNa_v1.1$	W1358S	EIEE6	DIII S5	W1332
$hNa_v1.1$	N1367K	EIEE6	DIII S5	N1341
$hNa_v1.1$	A1370P	EIEE6	DIII S5-S6	A1344
$hNa_v1.1$	N1378H	EIEE6	DIII S5-S6	N1352
$hNa_v1.1$	N1378T	EIEE6	DIII S5-S6	N1352
$hNa_v1.1$	F1385V	EIEE6	DIII S5-S6	F1359
$hNa_v1.1$	V1390M	EIEE6	DIII S5-S6	V1364
$hNa_v1.1$	N1391S	EIEE6	DIII S5-S6	P1365
$hNa_v1.1$	H1393P	EIEE6	DIII S5-S6	R1367
$hNa_v1.1$	T1394I	EIEE6	DIII S5-S6	S1368
$hNa_v1.1$	C1396G	EIEE6	DIII S5-S6	C1370
$hNa_v1.1$	C1396Y	EIEE6	DIII S5-S6	C1370
$hNa_v1.1$	N1414Y	EIEE6	DIII S5-S6	N1388
$hNa_v1.1$	D1416G	EIEE6	DIII S5-S6	D1390
$hNa_v1.1$	N1417S	EIEE6	DIII S5-S6	N1391
$hNa_v1.1$	V1418G	EIEE6	DIII S5-S6	V1392
$hNa_v1.1$	Y1422C	EIEE6	DIII S5-S6	Y1396
$hNa_v1.1$	L1423F	EIEE6	DIII S5-S6	L1397
$hNa_v1.1$	L1426R	EIEE6	DIII S5-S6	L1400
$hNa_v1.1$	Q1427P	EIEE6	DIII S5-S6	Q1401
$hNa_v1.1$	F1431I	EIEE6	DIII S5-S6	F1405
$hNa_v1.1$	G1433E	EIEE6	DIII S5-S6	G1407
$hNa_v1.1$	G1433R	EIEE6	DIII S5-S6	G1407
$hNa_v1.1$	G1433V	EIEE6	DIII S5-S6	G1407
$hNa_v1.1$	W1434R	EIEE6	DIII S5-S6	W1408
$hNa_v1.1$	I1437M	EIEE6	DIII S5-S6	I1411
$hNa_v1.1$	A1441P	EIEE6	DIII S5-S6	A1415
$hNa_v1.1$	Q1450K	EIEE6	DIII S5-S6	Q1424
$hNa_v1.1$	Q1450R	EIEE6	DIII S5-S6	Q1424
$hNa_v1.1$	P1451L	EIEE6	DIII S5-S6	P1425
$hNa_v1.1$	P1451S	EIEE6	DIII S5-S6	P1425
$hNa_v1.1$	Y1453C	EIEE6	DIII S5-S6	Y1427
$hNa_v1.1$	E1454K	EIEE6	DIII S5-S6	E1428
$hNa_v1.1$	L1461I	EIEE6	DIII S6	I1435
$hNa_v1.1$	Y1462C	EIEE6	DIII S6	Y1436

Table 2 continued

Related proteins	Mutations	Diseases	Structural position	Map on $hNa_v1.7$
$hNa_v1.1$	Y1462H	EIEE6	DIII S6	Y1436
$hNa_v1.1$	F1463S	EIEE6	DIII S6	F1437
$hNa_v1.1$	G1470W	EIEE6	DIII S6	G1444
$hNa_v1.1$	F1472S	EIEE6	DIII S6	F1446
$hNa_v1.1$	L1475S	EIEE6	DIII S6	L1449
$hNa_v1.1$	N1476K	EIEE6	DIII S6	N1450
$hNa_v1.1$	D1484G	EIEE6	DIII S6	D1458
$hNa_v1.1$	N1485Y	EIEE6	DIII S6	N1459
$hNa_v1.1$	E1503K	EIEE6	DIII - DIV	E1477
$hNa_v1.1$	L1514S	EIEE6	DIII - DIV	L1488
$hNa_v1.1$	V1538I	EIEE6	DIII - DIV	V1512
$hNa_v1.1$	D1544A	EIEE6	DIV S1	D1518
$hNa_v1.1$	D1544G	EIEE6	DIV S1	D1518
$hNa_v1.1$	I1545V	EIEE6	DIV S1	I1519
$hNa_v1.1$	M1555R	EIEE6	DIV S1	M1529
$hNa_v1.1$	E1561K	EIEE6	DIV S1-S2	E1535
$hNa_v1.1$	V1579E	EIEE6	DIV S2	V1553
$hNa_v1.1$	G1586E	EIEE6	DIV S2	G1560
$hNa_v1.1$	C1588R	EIEE6	DIV S2	C1562
$hNa_v1.1$	L1592H	EIEE6	DIV S2	L1566
$hNa_v1.1$	L1592P	EIEE6	DIV S2	L1566
$hNa_v1.1$	R1596C	EIEE6	DIV S2-S3	R1570
$hNa_v1.1$	R1596L	EIEE6	DIV S2-S3	R1570
$hNa_v1.1$	N1605S	EIEE6	DIV S3	N1579
$hNa_v1.1$	D1608G	EIEE6	DIV S3	D1582
$hNa_v1.1$	D1608Y	EIEE6	DIV S3	D1582
$hNa_v1.1$	V1612I	EIEE6	DIV S3	V1586
$hNa_v1.1$	V1630L	EIEE6	DIV S3-S4	V1604
$hNa_v1.1$	V1630M	EIEE6	DIV S3-S4	V1604
$hNa_v1.1$	V1637E	EIEE6	DIV S4	V1611
$hNa_v1.1$	I1638N	EIEE6	DIV S4	I1612
$hNa_v1.1$	I1638T	EIEE6	DIV S4	I1612
$hNa_v1.1$	R1639G	EIEE6	DIV S4	R1613
$hNa_v1.1$	R1642S	EIEE6	DIV S4	R1616
$hNa_v1.1$	R1645Q	EIEE6	DIV S4	R1619
$hNa_v1.1$	R1648C	EIEE6	DIV S4	R1622
$hNa_v1.1$	R1648H	EIEE6	DIV S4	R1622
$hNa_v1.1$	A1653E	EIEE6	DIV S4-S5	A1627
$hNa_v1.1$	T1658M	EIEE6	DIV S5	T1632
$hNa_v1.1$	T1658R	EIEE6	DIV S5	T1632
$hNa_v1.1$	L1660P	EIEE6	DIV S5	L1634
$hNa_v1.1$	F1661S	EIEE6	DIV S5	F1635

Table 2 continued

Related proteins	Mutations	Diseases	Structural position	Map on $hNa_v1.7$
$hNa_v1.1$	A1662V	EIEE6	DIV S5	A1636
$hNa_v1.1$	M1664K	EIEE6	DIV S5	M1638
$hNa_v1.1$	L1667P	EIEE6	DIV S5	L1641
$hNa_v1.1$	P1668A	EIEE6	DIV S5	P1642
$hNa_v1.1$	P1668L	EIEE6	DIV S5	P1642
$hNa_v1.1$	N1672I	EIEE6	DIV S5	N1646
$hNa_v1.1$	I1673T	EIEE6	DIV S5	I1647
$hNa_v1.1$	G1674R	EIEE6	DIV S5	G1648
$hNa_v1.1$	L1675R	EIEE6	DIV S5	L1649
$hNa_v1.1$	L1677F	EIEE6	DIV S5	L1651
$hNa_v1.1$	I1683T	EIEE6	DIV S5	I1657
$hNa_v1.1$	Y1684D	EIEE6	DIV S5	Y1658
$hNa_v1.1$	A1685D	EIEE6	DIV S5	A1659
$hNa_v1.1$	G1688W	EIEE6	DIV S5	G1662
$hNa_v1.1$	F1692S	EIEE6	DIV S5	F1666
$hNa_v1.1$	Y1694C	EIEE6	DIV S5-S6	Y1668
$hNa_v1.1$	F1707V	EIEE6	DIV S5-S6	F1681
$hNa_v1.1$	S1713N	EIEE6	DIV S5-S6	S1687
$hNa_v1.1$	M1714K	EIEE6	DIV S5-S6	M1688
$hNa_v1.1$	M1714R	EIEE6	DIV S5-S6	M1688
$hNa_v1.1$	C1716R	EIEE6	DIV S5-S6	C1690
$hNa_v1.1$	T1721R	EIEE6	DIV S5-S6	T1695
$hNa_v1.1$	G1725C	EIEE6	DIV S5-S6	G1699
$hNa_v1.1$	W1726R	EIEE6	DIV S5-S6	W1700
$hNa_v1.1$	D1727G	EIEE6	DIV S5-S6	D1701
$hNa_v1.1$	C1741R	EIEE6	DIV S5-S6	C1715
$hNa_v1.1$	G1749E	EIEE6	DIV S5-S6	G1723
$hNa_v1.1$	C1756G	EIEE6	DIV S5-S6	C1730
$hNa_v1.1$	G1762E	EIEE6	DIV S6	G1736
$hNa_v1.1$	I1763N	EIEE6	DIV S6	I1737
$hNa_v1.1$	I1770F	EIEE6	DIV S6	I1744
$hNa_v1.1$	I1770N	EIEE6	DIV S6	I1744
$hNa_v1.1$	I1770T	EIEE6	DIV S6	I1744
$hNa_v1.1$	I1771F	EIEE6	DIV S6	I1745
$hNa_v1.1$	I1771N	EIEE6	DIV S6	I1745
$hNa_v1.1$	S1773F	EIEE6	DIV S6	S1747
$hNa_v1.1$	M1780T	EIEE6	DIV S6	M1754
$hNa_v1.1$	Y1781C	EIEE6	DIV S6	Y1755
$hNa_v1.1$	Y1781H	EIEE6	DIV S6	Y1755
$hNa_v1.1$	I1782M	EIEE6	DIV S6	I1756
$hNa_v1.1$	I1782S	EIEE6	DIV S6	I1756
$hNa_v1.1$	A1783T	EIEE6	DIV S6	A1757

Table 2 continued

Related proteins	Mutations	Diseases	Structural position	Map on $hNa_v1.7$
$hNa_v1.1$	A1783V	EIEE6	DIV S6	A1757
$hNa_v1.1$	E1787K	EIEE6	DIV S6	E1761
$hNa_v1.1$	N1788K	EIEE6	DIV S6	N1862
$hNa_v1.1$	A1792T	EIEE6	C-terminus	A1766
$hNa_v1.1$	F1808I	EIEE6	C-terminus	F1782
$hNa_v1.1$	W1812G	EIEE6	C-terminus	W1786
$hNa_v1.1$	W1812S	EIEE6	C-terminus	W1786
$hNa_v1.1$	F1831S	EIEE6	C-terminus	F1805
$hNa_v1.1$	A1832P	EIEE6	C-terminus	A1806
$hNa_v1.1$	L1835F	EIEE6	C-terminus	L1809
$hNa_v1.1$	M1852K	EIEE6	C-terminus	M1826
$hNa_v1.1$	P1855L	EIEE6	C-terminus	P1829
$hNa_v1.1$	G1880E	EIEE6	C-terminus	G1854
$hNa_v1.1$	E1881D	EIEE6	C-terminus	E1855
$hNa_v1.1$	T1909I	EIEE6	C-terminus	T1883
$hNa_v1.1$	I1922T	EIEE6	C-terminus	I1896
$hNa_v1.1$	F90S	ICEGTC	N-terminus	F88
$hNa_v1.1$	R101Q	ICEGTC	N-terminus	R99
$hNa_v1.1$	F178S	ICEGTC	DI S2-S3	F176
$hNa_v1.1$	I252M	ICEGTC	DI S5	I250
$hNa_v1.1$	H290R	ICEGTC	DI S5-S6	S288
$hNa_v1.1$	R393H	ICEGTC	DI S5-S6	R372
$hNa_v1.1$	T808S	ICEGTC	DII S2	T784
$hNa_v1.1$	V896I	ICEGTC	DII S5	V872
$hNa_v1.1$	V944A	ICEGTC	DII S5-S6	R920
$hNa_v1.1$	G979R	ICEGTC	DII S6	G955
$hNa_v1.1$	V983A	ICEGTC	DII S6	V959
$hNa_v1.1$	N1011I	ICEGTC	DII - DIII	N987
$hNa_v1.1$	R1213Q	ICEGTC	DII - DIII	K1187
$hNa_v1.1$	Y1254C	ICEGTC	DIII S2	Y1228
$hNa_v1.1$	R1325T	ICEGTC	DIII S4	R1299
$hNa_v1.1$	S1328P	ICEGTC	DIII S4-S5	S1302
$hNa_v1.1$	F1357L	ICEGTC	DIII S5	F1331
$hNa_v1.1$	V1366I	ICEGTC	DIII S5	V1340
$hNa_v1.1$	C1376R	ICEGTC	DIII S5-S6	C1350
$hNa_v1.1$	A1429D	ICEGTC	DIII S5-S6	A1403
$hNa_v1.1$	Y1462H	ICEGTC	DIII S6	Y1436
$hNa_v1.1$	M1511K	ICEGTC	DIII - DIV	M1485
$hNa_v1.1$	V1611F	ICEGTC	DIV S3	V1585
$hNa_v1.1$	M1619V	ICEGTC	DIV S3	M1593
$hNa_v1.1$	P1632S	ICEGTC	DIV S3-S4	P1606
$hNa_v1.1$	Y1684S	ICEGTC	DIV S5	Y1658

Table 2 continued

Related proteins	Mutations	Diseases	Structural position	Map on $hNa_v1.7$
$hNa_v1.1$	T1709I	ICEGTC	DIV S5-S6	T1683
$hNa_v1.1$	A1724P	ICEGTC	DIV S5-S6	A1698
$hNa_v1.1$	Y1781C	ICEGTC	DIV S6	Y1755
$hNa_v1.1$	F1808L	ICEGTC	C-terminus	F1782
$hNa_v1.1$	R1861W	ICEGTC	C-terminus	R1835
$hNa_v1.1$	T1174S	FHM3	DII - DIII	S1148
$hNa_v1.1$	Q1489H	FHM3	DIII S6	Q1463
$hNa_v1.1$	Q1489K	FHM3	DIII S6	Q1463
$hNa_v1.1$	F1499L	FHM3	DIII - DIV	F1473
$hNa_v1.1$	L1649Q	FHM3	DIV S4	L1623
$hNa_v1.1$	M145T	FEB3A	DI S1	M143
$hNa_v1.1$	E1308D	FEB3A	DIII S3-S4	D1282

GEFS+2: Generalized epilepsy with febrile seizures plus 2; EIEE6: Epileptic encephalopathy, early infantile, 6; ICEGTC: Intractable childhood epilepsy with generalized tonic-clonic seizures; FHM3: Migraine, familial hemiplegic, 3; FEB3A: Febrile seizures, familial, 3A.

transmission (Djouhri et al., 2003; Dib-Hajj et al., 2013). Gain-of-function mutations of $Na_v1.7$ are implicated in two distinct paroxysmal pain syndromes—IEM (primary erythermalgia) and PEPD (paroxysmal extreme pain disorder), while loss-of-function mutations of $Na_v1.7$ inflict people with CIP (indifference to pain, congenital, autosomal recessive) (Lampert et al., 2010; Dib-Hajj et al., 2013). In all, Na_v channel mutations play a central role in the pathophysiology of sodium channelopathies. Pharmacologic modulation of Na_v channels may thereby represent a viable therapeutic approach for the treatment of many neurological disorders such as epilepsy, arrhythmia, and pain.

Despite significant advancement in the understanding of Na_v channel functions and their relevance to diseases, structural characterization of mammalian Na_v channels at atomic level has been challenging, partly due to the substantial technical hurdles in producing mammalian Na_v channel proteins in sufficient amount with acceptable purity. The two published bacterial Na_v channel crystal structures, Na_vAb (Payandeh et al., 2011) and Na_vRh (Zhang et al., 2012), in their full-length have greatly improved our understanding of how those channels conduct and select sodium ions on a structural basis. This is further enhanced by the recently published cryo-electron microscopy (cryo-EM) structure of the rabbit voltage-gated calcium (Ca_v) channel $Ca_v1.1$ (Wu et al., 2015; Wu et al., 2016), which, given the significant similarities between Ca_v and Na_v channels, provides an excellent base model for studying the structure and function of the mammalian Na_v channels in lieu of the elusive Na_v channel structure (Wu et al., 2015; Wu et al., 2016). In this Resource article, we have built a structure model of the human sodium channel $Na_v1.7$ based on the $Ca_v1.1$ cryo-EM structure (PDB code: 5GJV). Disease-related mutations of various Na_v channels are systematically mapped onto this $Na_v1.7$ structural model. As expected, most mutations are located in the VSDs and the pore domain, which corroborate the functional disturbance associated with the various conditions. The human $Na_v1.7$ structure model may also provide a useful tool for the structure-based design of drugs that are able to therapeutically target the Na_v channels.

STRUCTURE MODEL OF HUMAN SODIUM CHANNEL $NA_V1.7$

Homology models of the mammalian Na_v channels have been previously constructed based on the crystal structures of the eukaryotic potassium channels or the prokaryotic sodium channels (Tikhonov and Zhorov, 2012; Yang et al., 2012). However, the relevance of such models has been in question, since the eukaryotic sodium channels are known to be heterotetrameric while the prokaryotic sodium channels and the potassium channels are of homotetrameric nature.

We sought to build a homology-based structural model for human $Na_v1.7$ because of the tremendous interest in drug development targeting this channel. The sequence identity and similarity between human $Na_v1.7$ and rabbit $Ca_v1.1$ are 21 and 35%, respectively (Please refer to the online Supplementary Fig. 2 of Wu et al., 2016). Importantly, the key amino acids within the VSDs and the pore domains are highly conserved (Wu et al., 2015; Wu et al., 2016). The cryo-EM structure of rabbit $Ca_v1.1$ was then used as the template for homology modeling of human $Na_v1.7$. The primary sequence of human $Na_v1.7$ was aligned with rabbit

Table 3. Structural mapping of disease-related mutations identified in human $Na_v1.2$

Related proteins	Mutations	Diseases	Structural position	Map on $hNa_v1.7$
$hNa_v1.2$	E169G	EIEE11	DI S2	E166
$hNa_v1.2$	R188W	BFIS3	DI S3	R185
$hNa_v1.2$	V208E	BFIS3	DI S3-S4	V205
$hNa_v1.2$	N212D	EIEE11	DI S3-S4	N209
$hNa_v1.2$	V213D	EIEE11	DI S3-S4	V210
$hNa_v1.2$	R223Q	BFIS3	DI S4	R220
$hNa_v1.2$	T236S	EIEE11	DI S5	T233
$hNa_v1.2$	M252V	BFIS3	DI S5	M249
$hNa_v1.2$	V261M	BFIS3	DI S5	V258
$hNa_v1.2$	A263T	EIEE11	DI S5	A260
$hNa_v1.2$	A263V	EIEE11	DI S5	A260
$hNa_v1.2$	D322N	DS	DI - DII	D298
$hNa_v1.2$	F328V	DS	DI - DII	Y305
$hNa_v1.2$	E430Q	BFIS3	DI - DII	E407
$hNa_v1.2$	D649N	DS	DI - DII	D623
$hNa_v1.2$	R853Q	EIEE11	DII S4	R838
$hNa_v1.2$	N876T	EIEE11	DII S5	N861
$hNa_v1.2$	V892I	BFIS3	DII S5	V877
$hNa_v1.2$	E999K	EIEE11	DII - DIII	D984
$hNa_v1.2$	N1001K	BFIS3	DII - DIII	N986
$hNa_v1.2$	L1003I	BFIS3	DII - DIII	L988
$hNa_v1.2$	E1211K	EIEE11	DIII S1	E1195
$hNa_v1.2$	R1312T	EIEE11	DIII S4	R1296
$hNa_v1.2$	R1312T	DS	DIII S4	R1296
$hNa_v1.2$	R1319Q	BFIS3	DIII S4-S5	R1303
$hNa_v1.2$	M1323V	EIEE11	DIII S4-S5	M1307
$hNa_v1.2$	V1326L	EIEE11	DIII S4-S5	V1310
$hNa_v1.2$	V1326D	EIEE11	DIII S4-S5	V1310
$hNa_v1.2$	L1330F	BFIS3	DIII S4-S5	L1314
$hNa_v1.2$	S1336Y	EIEE11	DIII S4-S5	S1320
$hNa_v1.2$	M1338T	EIEE11	DIII S5	M1322
$hNa_v1.2$	L1342P	BFIS3	DIII S5	L1326
$hNa_v1.2$	I1473M	EIEE11	DIII S6	I1457
$hNa_v1.2$	L1563V	BFIS3	DIV S2	L1547
$hNa_v1.2$	Y1589C	BFIS3	DIV S2-S3	Y1573
$hNa_v1.2$	I1596S	BFIS3	DIV S3	I1580
$hNa_v1.2$	T1623N	EIEE11	DIV S3-S4	T1607
$hNa_v1.2$	R1629L	EIEE11	DIV S4	R1613
$hNa_v1.2$	L1660Y	EIEE11	DIV S5	L1644
$hNa_v1.2$	R1918H	BFIS3	C-terminus	R1902

BFIS3: Seizures, benign familial infantile 3; EIEE11: Epileptic encephalopathy, early infantile, 11; DS: Dravet syndrome.

Table 4. Structural mapping of disease-related mutations identified in human $Na_v1.3$

Related proteins	Mutations	Diseases	Structural position	Map on $hNa_v1.7$
$hNa_v1.3$	K354Q	CPE	DI - DII	K332
$hNa_v1.3$	R357Q	CPE	DI - DII	R335
$hNa_v1.3$	D815N	CPE	DII S2-S3	D799
$hNa_v1.3$	E1160K	CPE	DII - DIII	M1146
$hNa_v1.3$	M1372V	CPE	DIII S5-S6	R1358
$hNa_v1.3$	G1862C	CPE	C-terminus	G1851

CPE: Cryptogenic partial epilepsy.

$Ca_v1.1$ in MOE with manual adjustment when necessary. The structure model of human $Na_v1.7$ was created with the Homology Model module in MOE using the GB/VI scoring function with AMBER12:EHT force field (MOE, 2016).

The human $Na_v1.7$ model structure resembles the structure of $rCa_v1.1$ in general (Fig. 1A). However, the model exhibits pronounced differences from the calcium channel and bacterial sodium channels particularly in selectivity filter. The SF of $Na_v1.7$ consists of four different amino acid residues DEKA (Fig. 1B). In contrast, the $Ca_v1.1$ SF is constituted by four repeated essential glutamic acids, EEEE, while Na_vAb and Na_vRh contain TLESWS or TLSSWE in each protomer, respectively. This human $Na_v1.7$ structure model represents the first one-chain sodium channel model with asymmetric repeats and is expected to shed new light on the mammalian sodium channel functions.

MAPPING OF DISEASE-RELEVANT MUTATIONS ONTO THE $NA_V1.7$ STRUCTURE MODEL

Human $Na_v1.7$ sodium channel is preferentially expressed in the sensory neurons of dorsal root ganglia and sympathetic ganglia neurons, particularly within the nociceptors, which is essential for perceiving pain (Djouhri et al., 2003; Dib-Hajj et al., 2013). To date, about 60 mutations of $Na_v1.7$ have been found to cause human pain syndromes including IEM, PEPD, CIP, SFN (small fiber neuropathy), DS (Dravet syndrome), and FEB (febrile seizure) (Fig. 2 and Table 1). We mapped all the reported $Na_v1.7$ mutations onto this $Na_v1.7$ structure model (Fig. 2). Nineteen out of 22 IEM mutations are located in the highly conserved regions of VSDs and the pore domain except for the Q10R, P610T, and G616R mutations (Fig. 2). Electrophysiology study showed that IEM mutations cause a prominent shift of the activation voltage toward a more negative region or delay deactivation, which results in neuron hyperexcitability (Choi et al., 2006; Lampert et al., 2006; Choi et al., 2009; Lampert et al., 2010). For example, mutation of A1643 within the S5 segment of domain IV to glycine (A1643G) generates a significant hyperpolarizing shift (Yang et al., 2016). Our structural analysis shows that only two IEM mutations F216S and L834R are located in the S4 positively charged segment that is directly responsible for transmembrane voltage sensing and channel activation. How other IEM mutations influence voltage sensing and channel functions is yet to be elucidated.

The PEPD mutations are mostly characterized (nine out of 11) within the S4 segment, S4-S5 linker region, and the cytosolic regions of domain III and domain IV of $Na_v1.7$ except for R185H and R1007C (Fig. 2A and Table 1). Specifically, I1472T, F1473V, and T1475I are within the IFMT motif (Fig. 2A), indicating that they may disturb channel inactivation. Indeed, IFMT mutations usually impair fast inactivation with consequently persistent currents (Fertleman et al., 2006). The V1309D, V1309F, and V1310F mutations are located in the S4-S5 linker region of domain III and they have been shown to cause moderate destabilization of fast inactivation (Jarecki et al., 2008). The G1618R mutation, located within the S4 segment of domain IV, impairs inactivation and retains a persistent current compared to the wild-type (WT) channel (Choi et al., 2011), while another domain IV S4 segment mutation, L1623P, significantly increases ramp current and shortens recovery time from inactivation (Suter et al., 2015). Moreover, electrophysiology study showed that M1638K mutation (within the S5 segment of domain IV) generates faster recovery from inactivation than the WT channel, producing greater currents and reducing the threshold with increased number of action potentials (Fertleman et al., 2006; Dib-Hajj et al., 2008). Another PEPD mutation, A1643E, also located in the S5 segment of domain IV, impedes channel full inactivation, which results in persistent inward currents (Estacion et al., 2008).

The CIP patients, characterized by lack of nociceptive perception, are mostly inflicted by $Na_v1.7$ nonsense mutations, which result in premature protein truncations and inability to produce functional sodium channels. Only three mutations of $Na_v1.7$, namely R907Q, A1247E, and W1786R, have been reported to be associated with CIP (Fig. 2 and Table 1). Diseases such as DS, SFN, and FEB are also known to be caused by $Na_v1.7$ mutations (Fig. 2 and Table 1). For example, all eight SFN mutations have been characterized. Specifically, I228M, I731K, I750V, and M1543I mutations impair slow inactivation, D623N impedes slow and fast inactivation, while R185H, M943L, and V1002L mutations enhance resurgent currents (Faber et al., 2012a).

Table 5. Structural mapping of disease-related mutations identified in human $Na_v1.4$

Related proteins	Mutations	Diseases	Structural position	Map on $hNa_v1.7$
$hNa_v1.4$	Q270K	PMC	DI S5	Q265
$hNa_v1.4$	I693T	PMC	DII S5	I858
$hNa_v1.4$	T704M	PMC	DII S5	T870
$hNa_v1.4$	S804F	PMC	DII - DIII	S970
$hNa_v1.4$	A1152D	PMC	DIII S4-S5	A1313
$hNa_v1.4$	A1156T	PMC	DIII S4-S5	A1317
$hNa_v1.4$	V1293I	PMC	DIII S6	V1455
$hNa_v1.4$	G1306A	PMC	DIII S6	G1468
$hNa_v1.4$	G1306E	PMC	DIII S6	G1468
$hNa_v1.4$	G1306V	PMC	DIII S6	G1468
$hNa_v1.4$	T1313M	PMC	DIII - DIV	T1475
$hNa_v1.4$	L1433R	PMC	DIV S3	L1595
$hNa_v1.4$	L1436P	PMC	DIV S3	L1598
$hNa_v1.4$	R1448C	PMC	DIV S4	R1610
$hNa_v1.4$	R1448H	PMC	DIV S4	R1610
$hNa_v1.4$	R1448L	PMC	DIV S4	R1610
$hNa_v1.4$	G1456E	PMC	DIV S4	G1618
$hNa_v1.4$	F1473S	PMC	DIV S5	F1635
$hNa_v1.4$	V1589M	PMC	DIV S6	V1751
$hNa_v1.4$	F1705I	PMC	C-terminus	F1867
$hNa_v1.4$	R222W	HOKPP2	DI S4	E217
$hNa_v1.4$	R669H	HOKPP2	DII S4	R835
$hNa_v1.4$	R672C	HOKPP2	DII S4	R838
$hNa_v1.4$	R672G	HOKPP2	DII S4	R838
$hNa_v1.4$	R672H	HOKPP2	DII S4	R838
$hNa_v1.4$	R672S	HOKPP2	DII S4	R838
$hNa_v1.4$	R1129Q	HOKPP2	DIII S4	R1290
$hNa_v1.4$	R1132Q	HOKPP2	DIII S4	R1293
$hNa_v1.4$	R1135C	HOKPP2	DIII S4	R1296
$hNa_v1.4$	R1135H	HOKPP2	DIII S4	R1299
$hNa_v1.4$	P1158S	HOKPP2	DIII S4-S5	P1319
$hNa_v1.4$	T704M	HYPP	DII S5	T870
$hNa_v1.4$	V781I	HYPP	DII S6	V947
$hNa_v1.4$	A1156T	HYPP	DIII S4-S5	A1317
$hNa_v1.4$	L1433R	HYPP	DIV S3	L1595
$hNa_v1.4$	M1592V	HYPP	DIV S6	M1754
$hNa_v1.4$	R675G	NKPP	DII S4	R841
$hNa_v1.4$	R675Q	NKPP	DII S4	R841
$hNa_v1.4$	R675W	NKPP	DII S4	R841
$hNa_v1.4$	V781I	NKPP	DII S6	V947
$hNa_v1.4$	R1129Q	NKPP	DIII S4	R1290
$hNa_v1.4$	M1592V	NKPP	DIV S6	M1754
$hNa_v1.4$	I141V	MYOSCN4A	DI S1	I136

Table 5 continued

Related proteins	Mutations	Diseases	Structural position	Map on $hNa_v1.7$
$hNa_v1.4$	R225W	MYOSCN4A	DI S4	R220
$hNa_v1.4$	N440K	MYOSCN4A	DI S6	N395
$hNa_v1.4$	V445M	MYOSCN4A	DI - DII	V440
$hNa_v1.4$	E452K	MYOSCN4A	DI - DII	E447
$hNa_v1.4$	I588V	MYOSCN4A	DII S1	I754
$hNa_v1.4$	F671S	MYOSCN4A	DII S4	F837
$hNa_v1.4$	A715T	MYOSCN4A	DII S5	A881
$hNa_v1.4$	S804N	MYOSCN4A	DII - DIII	S970
$hNa_v1.4$	A1156T	MYOSCN4A	DIII S4-S5	A1317
$hNa_v1.4$	P1158L	MYOSCN4A	DIII S4-S5	P1319
$hNa_v1.4$	I1160V	MYOSCN4A	DIII S4-S5	I1321
$hNa_v1.4$	N1297K	MYOSCN4A	DIII S6	I1457
$hNa_v1.4$	G1306E	MYOSCN4A	DIII S6	G1468
$hNa_v1.4$	G1306V	MYOSCN4A	DIII S6	G1468
$hNa_v1.4$	I1310N	MYOSCN4A	DIII - DIV	I1472
$hNa_v1.4$	M1476I	MYOSCN4A	DIV S5	M1638
$hNa_v1.4$	A1481D	MYOSCN4A	DIV S5	A1643
$hNa_v1.4$	Q1633E	MYOSCN4A	C-terminus	Q1795
$hNa_v1.4$	R104H	CMS16	N-terminus	R99
$hNa_v1.4$	M203K	CMS16	DI S3	F198
$hNa_v1.4$	R225W	CMS16	DI S4	R220
$hNa_v1.4$	S246L	CMS16	DI S5	S241
$hNa_v1.4$	P382T	CMS16	DI S5-S6	P337
$hNa_v1.4$	D1069N	CMS16	DIII S2	D1230
$hNa_v1.4$	R1135C	CMS16	DIII S4-S5	R1299
$hNa_v1.4$	C1209F	CMS16	DIII S5-S6	C1370
$hNa_v1.4$	V1442E	CMS16	DIV S3-S4	V1604
$hNa_v1.4$	R1454W	CMS16	DIV S4	R1616
$hNa_v1.4$	R1457H	CMS16	DIV S4	R1619

PMC: Paramyotonia congenita of von Eulenburg; HOKPP2: Periodic paralysis hypokalemic 2; HYPP: Periodic paralysis hyperkalemic; NKPP: Periodic paralysis normokalemic; MYOSCN4A: Myotonia SCN4A-related; CMS16: Myasthenic syndrome, congenital, 16.

On the other hand, $Na_v1.7$ mutations that are associated with DS (nine mutations) and FEB (six mutations) have not been well characterized.

MAPPING OF OTHER HUMAN SODIUM CHANNEL DISEASE-RELATED MUTATIONS ONTO THE $NA_V1.7$ STRUCTURE MODEL

Members of the human Na_v channel family share high sequence similarity and mutations of these Na_v channels are known to cause a vast variety of channelopathies. In order to better understand the role of those mutations in disturbing normal channel functions on a structural level, we mapped the disease-related mutations of other human Na_v channels onto the $Na_v1.7$ structure model based on the sequence alignment reported in Wu et al., 2016 (Fig. 3).

Among all the nine Na_v channels, $Na_v1.1$ and $Na_v1.5$ have the largest numbers of reported mutations (more than 400 each) (Fig. 3A and 3E), while $Na_v1.3$, $Na_v1.8$, and $Na_v1.9$ have the least numbers (less than 10 each) (Fig. 3C, 3H, and 3I). Notably, mutations in $Na_v1.1$, $Na_v1.2$, $Na_v1.3$, and $Na_v1.6$ mainly cause epilepsies; those in $Na_v1.4$ are related to myopathies; in $Na_v1.5$ result in cardiac

Table 6. Structural mapping of disease-related mutations identified in human $Na_v1.5$

Related proteins	Mutations	Diseases	Structural position	Map on $hNa_v1.7$
$hNa_v1.5$	E161K	PFHB1A	DI S2	E156
$hNa_v1.5$	R225W	PFHB1A	DI S4	R220
$hNa_v1.5$	G298S	PFHB1A	DI S4-S5	–
$hNa_v1.5$	T512I	PFHB1A	DI - DII	V518
$hNa_v1.5$	G514C	PFHB1A	DI - DII	G520
$hNa_v1.5$	G752R	PFHB1A	DII S2-S3	G779
$hNa_v1.5$	R1232W	PFHB1A	DIII S1-S2	K1219
$hNa_v1.5$	D1275N	PFHB1A	DIII S3	D1262
$hNa_v1.5$	D1595N	PFHB1A	DIII D3-S4	D1582
$hNa_v1.5$	T1620K	PFHB1A	DIV S3-S4	T1607
$hNa_v1.5$	G9V	LQT3	N-terminus	G8
$hNa_v1.5$	R18Q	LQT3	N-terminus	K17
$hNa_v1.5$	R27H	LQT3	N-terminus	R26
$hNa_v1.5$	E30G	LQT3	N-terminus	E29
$hNa_v1.5$	R43Q	LQT3	N-terminus	K40
$hNa_v1.5$	E48K	LQT3	N-terminus	D43
$hNa_v1.5$	P52S	LQT3	N-terminus	P47
$hNa_v1.5$	R53Q	LQT3	N-terminus	K48
$hNa_v1.5$	R104G	LQT3	N-terminus	R99
$hNa_v1.5$	S115G	LQT3	N-terminus	S110
$hNa_v1.5$	V125L	LQT3	N-terminus	I125
$hNa_v1.5$	L212P	LQT3	DI S3-S4	L207
$hNa_v1.5$	R222Q	LQT3	DI S4	R217
$hNa_v1.5$	R225Q	LQT3	DI S4	R220
$hNa_v1.5$	R225W	LQT3	DI S4	R220
$hNa_v1.5$	V240M	LQT3	DI S5	V235
$hNa_v1.5$	Q245K	LQT3	DI S5	Q240
$hNa_v1.5$	V247L	LQT3	DI S5	L242
$hNa_v1.5$	N275K	LQT3	DI S5-S6	N270
$hNa_v1.5$	G289S	LQT3	DI S5-S6	E284
$hNa_v1.5$	R340W	LQT3	DI S5-S6	T329
$hNa_v1.5$	R367C	LQT3	DI S5-S6	R356
$hNa_v1.5$	T370M	LQT3	DI S5-S6	T359
$hNa_v1.5$	I397T	LQT3	DI S6	I386
$hNa_v1.5$	L404Q	LQT3	DI S6	L393
$hNa_v1.5$	N406K	LQT3	DI S6	N395
$hNa_v1.5$	L409V	LQT3	DI S6	L398
$hNa_v1.5$	V411M	LQT3	DI S6	V400
$hNa_v1.5$	A413E	LQT3	DI S6	A402
$hNa_v1.5$	A413T	LQT3	DI S6	A402
$hNa_v1.5$	E462A	LQT3	DI - DII	E464
$hNa_v1.5$	E462K	LQT3	DI - DII	E464
$hNa_v1.5$	F530V	LQT3	DI - DII	F555

Table 6 continued

Related proteins	Mutations	Diseases	Structural position	Map on $hNa_v1.7$
$hNa_v1.5$	R535Q	LQT3	DI - DII	R562
$hNa_v1.5$	R569W	LQT3	DI - DII	E596
$hNa_v1.5$	S571I	LQT3	DI - DII	R598
$hNa_v1.5$	A572D	LQT3	DI - DII	S599
$hNa_v1.5$	A572S	LQT3	DI - DII	S599
$hNa_v1.5$	A572V	LQT3	DI - DII	S599
$hNa_v1.5$	Q573E	LQT3	DI - DII	S600
$hNa_v1.5$	G579R	LQT3	DI - DII	S606
$hNa_v1.5$	G615E	LQT3	DI - DII	N641
$hNa_v1.5$	L619F	LQT3	DI - DII	L615
$hNa_v1.5$	P637L	LQT3	DI - DII	–
$hNa_v1.5$	G639R	LQT3	DI - DII	K666
$hNa_v1.5$	P648L	LQT3	DI - DII	L675
$hNa_v1.5$	E654K	LQT3	DI - DII	N681
$hNa_v1.5$	L673P	LQT3	DI - DII	V700
$hNa_v1.5$	R680H	LQT3	DI - DII	Q708
$hNa_v1.5$	R689C	LQT3	DI - DII	R716
$hNa_v1.5$	R689H	LQT3	DI - DII	R716
$hNa_v1.5$	P701L	LQT3	DI - DII	P728
$hNa_v1.5$	T731I	LQT3	DII S1	T758
$hNa_v1.5$	Q750R	LQT3	DII S2	A777
$hNa_v1.5$	D772N	LQT3	DII S2-S3	D799
$hNa_v1.5$	F816Y	LQT3	DII S4	F843
$hNa_v1.5$	I848F	LQT3	DII S5	I875
$hNa_v1.5$	S941N	LQT3	DII - DIII	S970
$hNa_v1.5$	Q960K	LQT3	DII - DIII	Q989
$hNa_v1.5$	R965L	LQT3	DII - DIII	R994
$hNa_v1.5$	R971C	LQT3	DII - DIII	N1000
$hNa_v1.5$	C981F	LQT3	DII - DIII	–
$hNa_v1.5$	A997S	LQT3	DII - DIII	E1023
$hNa_v1.5$	C1004R	LQT3	DII - DIII	Y1037
$hNa_v1.5$	E1053K	LQT3	DII - DIII	E1095
$hNa_v1.5$	T1069M	LQT3	DII - DIII	D1111
$hNa_v1.5$	A1100V	LQT3	DII - DIII	–
$hNa_v1.5$	D1114N	LQT3	DII - DIII	–
$hNa_v1.5$	D1166N	LQT3	DII - DIII	A1153
$hNa_v1.5$	R1193Q	LQT3	DII - DIII	N1180
$hNa_v1.5$	Y1199S	LQT3	DII - DIII	Y1186
$hNa_v1.5$	E1225K	LQT3	DIII S1-S2	E1212
$hNa_v1.5$	E1231K	LQT3	DIII S1-S2	R1218
$hNa_v1.5$	F1250L	LQT3	DIII S2	F1237
$hNa_v1.5$	L1283M	LQT3	DIII S3	L1270

Table 6 continued

Related proteins	Mutations	Diseases	Structural position	Map on $hNa_v1.7$
$hNa_v1.5$	E1295K	LQT3	DIII S3-S4	D1282
$hNa_v1.5$	T1304M	LQT3	DIII S4	T1291
$hNa_v1.5$	N1325S	LQT3	DIII S4-S5	N1312
$hNa_v1.5$	A1326S	LQT3	DIII S4-S5	A1313
$hNa_v1.5$	A1330P	LQT3	DIII S4-S5	A1317
$hNa_v1.5$	A1330T	LQT3	DIII S4-S5	A1317
$hNa_v1.5$	P1332L	LQT3	DIII S4-S5	P1319
$hNa_v1.5$	S1333Y	LQT3	DIII S4-S5	S1320
$hNa_v1.5$	I1334V	LQT3	DIII S4-S5	I1321
$hNa_v1.5$	L1338V	LQT3	DIII S5	L1325
$hNa_v1.5$	R1432S	LQT3	DIII S5-S6	V1419
$hNa_v1.5$	S1458Y	LQT3	DIII S6	S1445
$hNa_v1.5$	N1472S	LQT3	DIII S6	N1459
$hNa_v1.5$	F1473C	LQT3	DIII S6	F1460
$hNa_v1.5$	G1481E	LQT3	DIII - DIV	G1468
$hNa_v1.5$	F1486L	LQT3	DIII - DIV	F1473
$hNa_v1.5$	M1487L	LQT3	DIII - DIV	M1474
$hNa_v1.5$	T1488R	LQT3	DIII - DIV	T1475
$hNa_v1.5$	E1489D	LQT3	DIII - DIV	E1476
$hNa_v1.5$	K1493R	LQT3	DIII - DIV	K1480
$hNa_v1.5$	Y1495S	LQT3	DIII - DIV	Y1482
$hNa_v1.5$	M1498V	LQT3	DIII - DIV	M1485
$hNa_v1.5$	L1501V	LQT3	DIII - DIV	L1488
$hNa_v1.5$	K1505N	LQT3	DIII - DIV	K1492
$hNa_v1.5$	V1532I	LQT3	DIV S1	I1519
$hNa_v1.5$	L1560F	LQT3	DIV S2	L1547
$hNa_v1.5$	I1593M	LQT3	DIV S3	I1580
$hNa_v1.5$	F1594S	LQT3	DIV S3	F1581
$hNa_v1.5$	D1595N	LQT3	DIV S3	D1582
$hNa_v1.5$	F1596I	LQT3	DIV S3	F1583
$hNa_v1.5$	S1609W	LQT3	DIV S3	A1596
$hNa_v1.5$	T1620K	LQT3	DIV S3-S4	T1607
$hNa_v1.5$	R1623L	LQT3	DIV S4	R1610
$hNa_v1.5$	R1623Q	LQT3	DIV S4	R1610
$hNa_v1.5$	R1626H	LQT3	DIV S4	R1613
$hNa_v1.5$	R1626P	LQT3	DIV S4	R1613
$hNa_v1.5$	R1644C	LQT3	DIV S5	R1631
$hNa_v1.5$	R1644H	LQT3	DIV S5	R1631
$hNa_v1.5$	T1645M	LQT3	DIV S5	T1632
$hNa_v1.5$	L1650F	LQT3	DIV S5	L1637
$hNa_v1.5$	M1652R	LQT3	DIV S5	M1639
$hNa_v1.5$	M1652T	LQT3	DIV S5	M1639

Table 6 continued

Related proteins	Mutations	Diseases	Structural position	Map on $hNa_v1.7$
$hNa_v1.5$	I1660V	LQT3	DIV S5	I1647
$hNa_v1.5$	V1667I	LQT3	DIV S5	V1654
$hNa_v1.5$	T1723N	LQT3	DIV S5-S6	S1710
$hNa_v1.5$	R1739W	LQT3	DIV S5-S6	E1727
$hNa_v1.5$	L1761F	LQT3	DIV S6	L1749
$hNa_v1.5$	L1761H	LQT3	DIV S6	L1749
$hNa_v1.5$	V1763M	LQT3	DIV S6	V1751
$hNa_v1.5$	M1766L	LQT3	DIV S6	M1754
$hNa_v1.5$	Y1767C	LQT3	DIV S6	Y1755
$hNa_v1.5$	I1768V	LQT3	DIV S6	I1756
$hNa_v1.5$	V1777M	LQT3	C-terminus	V1765
$hNa_v1.5$	T1779M	LQT3	C-terminus	T1767
$hNa_v1.5$	E1784K	LQT3	C-terminus	E1772
$hNa_v1.5$	D1790G	LQT3	C-terminus	D1778
$hNa_v1.5$	Y1795C	LQT3	C-terminus	Y1783
$hNa_v1.5$	Y1795YD	LQT3	C-terminus	Y1783
$hNa_v1.5$	D1819N	LQT3	C-terminus	A1807
$hNa_v1.5$	L1825P	LQT3	C-terminus	L1813
$hNa_v1.5$	R1826H	LQT3	C-terminus	L1814
$hNa_v1.5$	D1839G	LQT3	C-terminus	D1827
$hNa_v1.5$	R1897W	LQT3	C-terminus	K1885
$hNa_v1.5$	E1901Q	LQT3	C-terminus	E1889
$hNa_v1.5$	S1904L	LQT3	C-terminus	S1892
$hNa_v1.5$	Q1909R	LQT3	C-terminus	Q1897
$hNa_v1.5$	R1913H	LQT3	C-terminus	R1901
$hNa_v1.5$	A1949S	LQT3	C-terminus	F1934
$hNa_v1.5$	V1951L	LQT3	C-terminus	N1936
$hNa_v1.5$	Y1977N	LQT3	C-terminus	Y1958
$hNa_v1.5$	F2004L	LQT3	C-terminus	D1982
$hNa_v1.5$	F2004V	LQT3	C-terminus	D1982
$hNa_v1.5$	R2012C	LQT3	C-terminus	–
$hNa_v1.5$	R18Q	BRGDA1	N-terminus	K17
$hNa_v1.5$	R27H	BRGDA1	N-terminus	R26
$hNa_v1.5$	N70K	BRGDA1	N-terminus	D65
$hNa_v1.5$	D84N	BRGDA1	N-terminus	D79
$hNa_v1.5$	F93S	BRGDA1	N-terminus	F88
$hNa_v1.5$	I94S	BRGDA1	N-terminus	I89
$hNa_v1.5$	V95I	BRGDA1	N-terminus	V90
$hNa_v1.5$	R104Q	BRGDA1	N-terminus	R99
$hNa_v1.5$	R104W	BRGDA1	N-terminus	R99
$hNa_v1.5$	N109K	BRGDA1	N-terminus	P104
$hNa_v1.5$	R121Q	BRGDA1	N-terminus	R116

Table 6 continued

Related proteins	Mutations	Diseases	Structural position	Map on $hNa_v1.7$
$hNa_v1.5$	R121W	BRGDA1	N-terminus	R116
$hNa_v1.5$	K126E	BRGDA1	N-terminus	K121
$hNa_v1.5$	L136P	BRGDA1	DI S1	L131
$hNa_v1.5$	V146M	BRGDA1	DI S1	I141
$hNa_v1.5$	E161K	BRGDA1	DI S2	E156
$hNa_v1.5$	E161Q	BRGDA1	DI S2	E156
$hNa_v1.5$	K175N	BRGDA1	DI S2	K170
$hNa_v1.5$	A178G	BRGDA1	DI S2-S3	A173
$hNa_v1.5$	C182R	BRGDA1	DI S2-S3	C177
$hNa_v1.5$	A185V	BRGDA1	DI S2-S3	E180
$hNa_v1.5$	T187I	BRGDA1	DI S3	T182
$hNa_v1.5$	A204V	BRGDA1	DI S3	A199
$hNa_v1.5$	L212Q	BRGDA1	DI S3-S4	L207
$hNa_v1.5$	T220I	BRGDA1	DI S4	T215
$hNa_v1.5$	R222Q	BRGDA1	DI S4	R217
$hNa_v1.5$	V223L	BRGDA1	DI S4	V218
$hNa_v1.5$	R225W	BRGDA1	DI S4	R220
$hNa_v1.5$	A226V	BRGDA1	DI S4	A221
$hNa_v1.5$	I230V	BRGDA1	DI S4	T225
$hNa_v1.5$	V232I	BRGDA1	DI S4	V227
$hNa_v1.5$	V240M	BRGDA1	DI S5	V235
$hNa_v1.5$	Q270K	BRGDA1	DI S5	Q265
$hNa_v1.5$	L276Q	BRGDA1	DI S5-S6	L271
$hNa_v1.5$	H278D	BRGDA1	DI S5-S6	H273
$hNa_v1.5$	R282C	BRGDA1	DI S5-S6	R277
$hNa_v1.5$	R282H	BRGDA1	DI S5-S6	R277
$hNa_v1.5$	V294M	BRGDA1	DI S5-S6	I289
$hNa_v1.5$	V300I	BRGDA1	DI S5-S6	–
$hNa_v1.5$	L315P	BRGDA1	DI S5-S6	Y304
$hNa_v1.5$	G319S	BRGDA1	DI S5-S6	G308
$hNa_v1.5$	T320N	BRGDA1	DI S5-S6	S319
$hNa_v1.5$	L325R	BRGDA1	DI S5-S6	L314
$hNa_v1.5$	P336L	BRGDA1	DI S5-S6	P325
$hNa_v1.5$	G351D	BRGDA1	DI S5-S6	G340
$hNa_v1.5$	G351V	BRGDA1	DI S5-S6	G340
$hNa_v1.5$	T353I	BRGDA1	DI S5-S6	T342
$hNa_v1.5$	D356N	BRGDA1	DI S5-S6	D345
$hNa_v1.5$	R367C	BRGDA1	DI S5-S6	R356
$hNa_v1.5$	R367H	BRGDA1	DI S5-S6	R356
$hNa_v1.5$	R367L	BRGDA1	DI S5-S6	R356
$hNa_v1.5$	M369K	BRGDA1	DI S5-S6	M358
$hNa_v1.5$	W374G	BRGDA1	DI S5-S6	W363

Table 6 continued

Related proteins	Mutations	Diseases	Structural position	Map on $hNa_v1.7$
$hNa_v1.5$	R376H	BRGDA1	DI S5-S6	N365
$hNa_v1.5$	G386E	BRGDA1	DI S5-S6	G375
$hNa_v1.5$	G386R	BRGDA1	DI S5-S6	G375
$hNa_v1.5$	V396A	BRGDA1	DI S6	V385
$hNa_v1.5$	V396L	BRGDA1	DI S6	V385
$hNa_v1.5$	N406S	BRGDA1	DI S6	N395
$hNa_v1.5$	E439K	BRGDA1	DI - DII	D428
$hNa_v1.5$	D501G	BRGDA1	DI - DII	D507
$hNa_v1.5$	G514C	BRGDA1	DI - DII	G520
$hNa_v1.5$	R526H	BRGDA1	DI - DII	R540
$hNa_v1.5$	F532C	BRGDA1	DI - DII	A546
$hNa_v1.5$	F543L	BRGDA1	DI - DII	F570
$hNa_v1.5$	G552R	BRGDA1	DI - DII	G579
$hNa_v1.5$	L567Q	BRGDA1	DI - DII	P594
$hNa_v1.5$	G615E	BRGDA1	DI - DII	N641
$hNa_v1.5$	L619F	BRGDA1	DI - DII	L615
$hNa_v1.5$	R620C	BRGDA1	DI - DII	E647
$hNa_v1.5$	T632M	BRGDA1	DI - DII	G659
$hNa_v1.5$	P640A	BRGDA1	DI - DII	K667
$hNa_v1.5$	A647D	BRGDA1	DI - DII	L674
$hNa_v1.5$	P648L	BRGDA1	DI - DII	L675
$hNa_v1.5$	R661W	BRGDA1	DI - DII	R688
$hNa_v1.5$	H681P	BRGDA1	DI - DII	Q708
$hNa_v1.5$	C683G	BRGDA1	DI - DII	C710
$hNa_v1.5$	P701L	BRGDA1	DI - DII	P728
$hNa_v1.5$	P717L	BRGDA1	DI - DII	P744
$hNa_v1.5$	A735E	BRGDA1	DII S1-S2	A762
$hNa_v1.5$	A735V	BRGDA1	DII S1-S2	A762
$hNa_v1.5$	E746K	BRGDA1	DII S2	K773
$hNa_v1.5$	G752R	BRGDA1	DII S2	G779
$hNa_v1.5$	G758E	BRGDA1	DII S2	G785
$hNa_v1.5$	M764R	BRGDA1	DII S2	M791
$hNa_v1.5$	D772N	BRGDA1	DII S2-S3	D799
$hNa_v1.5$	P773S	BRGDA1	DII S2-S3	P800
$hNa_v1.5$	V789I	BRGDA1	DII S3	V816
$hNa_v1.5$	R808P	BRGDA1	DII S4	R835
$hNa_v1.5$	R814Q	BRGDA1	DII S4	R841
$hNa_v1.5$	L839P	BRGDA1	DII S6	L866
$hNa_v1.5$	F851L	BRGDA1	DII S6	F878
$hNa_v1.5$	E867Q	BRGDA1	DII S5-S6	E894
$hNa_v1.5$	R878C	BRGDA1	DII S5-S6	R907
$hNa_v1.5$	R878H	BRGDA1	DII S5-S6	R907

Table 6 continued

Related proteins	Mutations	Diseases	Structural position	Map on $hNa_v1.7$
$hNa_v1.5$	H886P	BRGDA1	DII S5-S6	H915
$hNa_v1.5$	F892I	BRGDA1	DII S5-S6	F921
$hNa_v1.5$	R893C	BRGDA1	DII S5-S6	R922
$hNa_v1.5$	R893H	BRGDA1	DII S5-S6	R922
$hNa_v1.5$	C896S	BRGDA1	DII S5-S6	C925
$hNa_v1.5$	E901K	BRGDA1	DII S5-S6	E930
$hNa_v1.5$	S910L	BRGDA1	DII S5-S6	A939
$hNa_v1.5$	C915R	BRGDA1	DII S5-S6	C944
$hNa_v1.5$	L917R	BRGDA1	DII S6	I946
$hNa_v1.5$	N927S	BRGDA1	DII S6	N956
$hNa_v1.5$	L928P	BRGDA1	DII S6	L957
$hNa_v1.5$	L935P	BRGDA1	DII S6	L964
$hNa_v1.5$	R965C	BRGDA1	DII - DIII	R994
$hNa_v1.5$	R965H	BRGDA1	DII - DIII	R994
$hNa_v1.5$	A997T	BRGDA1	DII - DIII	Q1026
$hNa_v1.5$	R1023H	BRGDA1	DII - DIII	H1050
$hNa_v1.5$	E1053K	BRGDA1	DII - DIII	E1095
$hNa_v1.5$	D1055G	BRGDA1	DII - DIII	D1097
$hNa_v1.5$	S1079Y	BRGDA1	DII - DIII	–
$hNa_v1.5$	A1113V	BRGDA1	DII - DIII	–
$hNa_v1.5$	S1140T	BRGDA1	DII - DIII	S1128
$hNa_v1.5$	R1193Q	BRGDA1	DII - DIII	N1180
$hNa_v1.5$	S1219N	BRGDA1	DIII S1	S1206
$hNa_v1.5$	E1225K	BRGDA1	DIII S1-S2	E1212
$hNa_v1.5$	Y1228H	BRGDA1	DIII S1-S2	Y1215
$hNa_v1.5$	R1232Q	BRGDA1	DIII S1-S2	K1219
$hNa_v1.5$	R1232W	BRGDA1	DIII S1-S2	K1219
$hNa_v1.5$	K1236N	BRGDA1	DIII S2	K1223
$hNa_v1.5$	L1339P	BRGDA1	DIII S2	L1226
$hNa_v1.5$	E1240Q	BRGDA1	DIII S2	E1227
$hNa_v1.5$	D1243N	BRGDA1	DIII S2	D1230
$hNa_v1.5$	V1249D	BRGDA1	DIII S2	I1236
$hNa_v1.5$	E1253G	BRGDA1	DIII S2	E1240
$hNa_v1.5$	G1262S	BRGDA1	DIII S2-S3	G1249
$hNa_v1.5$	W1271C	BRGDA1	DIII S3	W1258
$hNa_v1.5$	D1275N	BRGDA1	DIII S3	D1262
$hNa_v1.5$	A1288G	BRGDA1	DIII S3-S4	A1275
$hNa_v1.5$	F1293S	BRGDA1	DIII S3-S4	Y1280
$hNa_v1.5$	L1311P	BRGDA1	DIII S4	L1298
$hNa_v1.5$	G1319V	BRGDA1	DIII S4-S5	G1306
$hNa_v1.5$	V1323G	BRGDA1	DIII S4-S5	V1310
$hNa_v1.5$	P1332L	BRGDA1	DIII S4-S5	P1319

Table 6 continued

Related proteins	Mutations	Diseases	Structural position	Map on $hNa_v1.7$
$hNa_v1.5$	F1344L	BRGDA1	DIII S5	F1331
$hNa_v1.5$	F1344S	BRGDA1	DIII S5	F1331
$hNa_v1.5$	L1346I	BRGDA1	DIII S5	L1333
$hNa_v1.5$	L1346P	BRGDA1	DIII S5	L1333
$hNa_v1.5$	M1351R	BRGDA1	DIII S5	M1338
$hNa_v1.5$	V1353M	BRGDA1	DIII S5	V1340
$hNa_v1.5$	G1358W	BRGDA1	DIII S5-S6	G1345
$hNa_v1.5$	K1359N	BRGDA1	DIII S5-S6	K1346
$hNa_v1.5$	F1360C	BRGDA1	DIII S5-S6	F1347
$hNa_v1.5$	C1363Y	BRGDA1	DIII S5-S6	C1350
$hNa_v1.5$	S1382I	BRGDA1	DIII S5-S6	E1369
$hNa_v1.5$	V1405L	BRGDA1	DIII S5-S6	V1392
$hNa_v1.5$	V1405M	BRGDA1	DIII S5-S6	V1392
$hNa_v1.5$	G1406E	BRGDA1	DIII S5-S6	G1393
$hNa_v1.5$	G1406R	BRGDA1	DIII S5-S6	G1393
$hNa_v1.5$	G1408R	BRGDA1	DIII S5-S6	G1395
$hNa_v1.5$	Y1409C	BRGDA1	DIII S5-S6	Y1396
$hNa_v1.5$	L1412F	BRGDA1	DIII S5-S6	L1399
$hNa_v1.5$	K1419E	BRGDA1	DIII S5-S6	K1406
$hNa_v1.5$	G1420R	BRGDA1	DIII S5-S6	G1407
$hNa_v1.5$	A1427S	BRGDA1	DIII S5-S6	A1414
$hNa_v1.5$	A1428V	BRGDA1	DIII S5-S6	A1415
$hNa_v1.5$	R1432G	BRGDA1	DIII S5-S6	V1419
$hNa_v1.5$	R1432S	BRGDA1	DIII S5-S6	V1419
$hNa_v1.5$	G1433V	BRGDA1	DIII S5-S6	N1420
$hNa_v1.5$	P1438L	BRGDA1	DIII S5-S6	P1425
$hNa_v1.5$	E1441Q	BRGDA1	DIII S5-S6	E1428
$hNa_v1.5$	I1448L	BRGDA1	DIII S6	I1435
$hNa_v1.5$	I1448T	BRGDA1	DIII S6	I1435
$hNa_v1.5$	Y1449C	BRGDA1	DIII S6	Y1436
$hNa_v1.5$	V1451D	BRGDA1	DIII S6	V1438
$hNa_v1.5$	N1463Y	BRGDA1	DIII S6	N1450
$hNa_v1.5$	V1468F	BRGDA1	DIII S6	V1455
$hNa_v1.5$	Y1494N	BRGDA1	DIII - DIV	Y1481
$hNa_v1.5$	L1501V	BRGDA1	DIII - DIV	L1488
$hNa_v1.5$	G1502S	BRGDA1	DIII - DIV	G1489
$hNa_v1.5$	R1512W	BRGDA1	DIII - DIV	R1499
$hNa_v1.5$	I1521K	BRGDA1	DIII - DIV	I1508
$hNa_v1.5$	V1525M	BRGDA1	DIII - DIV	V1512
$hNa_v1.5$	K1527R	BRGDA1	DIII - DIV	N1514
$hNa_v1.5$	E1548K	BRGDA1	DIV S1-S2	E1535
$hNa_v1.5$	A1569P	BRGDA1	DIV S2	I1556

Table 6 continued

Related proteins	Mutations	Diseases	Structural position	Map on $hNa_v1.7$
$hNa_v1.5$	F1571C	BRGDA1	DIV S2	F1558
$hNa_v1.5$	E1574K	BRGDA1	DIV S2	E1561
$hNa_v1.5$	L1582P	BRGDA1	DIV S2-S3	L1569
$hNa_v1.5$	R1583C	BRGDA1	DIV S2-S3	R1570
$hNa_v1.5$	R1583H	BRGDA1	DIV S2-S3	R1570
$hNa_v1.5$	V1604M	BRGDA1	DIV S3	V1591
$hNa_v1.5$	Q1613L	BRGDA1	DIV S3-S4	E1600
$hNa_v1.5$	T1620M	BRGDA1	DIV S3-S4	T1607
$hNa_v1.5$	R1623Q	BRGDA1	DIV S4	R1610
$hNa_v1.5$	R1629Q	BRGDA1	DIV S4	R1616
$hNa_v1.5$	G1642E	BRGDA1	DIV S5	G1629
$hNa_v1.5$	R1644C	BRGDA1	DIV S5	R1631
$hNa_v1.5$	A1649V	BRGDA1	DIV S5	A1636
$hNa_v1.5$	I1660V	BRGDA1	DIV S5	I1647
$hNa_v1.5$	G1661R	BRGDA1	DIV S5	G1648
$hNa_v1.5$	V1667I	BRGDA1	DIV S5	V1654
$hNa_v1.5$	S1672Y	BRGDA1	DIV S5	A1659
$hNa_v1.5$	A1680T	BRGDA1	DIV S5-S6	A1667
$hNa_v1.5$	A1698T	BRGDA1	DIV S5-S6	G1685
$hNa_v1.5$	T1709M	BRGDA1	DIV S5-S6	T1696
$hNa_v1.5$	T1709R	BRGDA1	DIV S5-S6	T1696
$hNa_v1.5$	G1712S	BRGDA1	DIV S5-S6	G1699
$hNa_v1.5$	D1714G	BRGDA1	DIV S5-S6	D1701
$hNa_v1.5$	N1722D	BRGDA1	DIV S5-S6	N1709
$hNa_v1.5$	C1728R	BRGDA1	DIV S5-S6	C1715
$hNa_v1.5$	C1728W	BRGDA1	DIV S5-S6	C1715
$hNa_v1.5$	G1740R	BRGDA1	DIV S5-S6	G1728
$hNa_v1.5$	G1743E	BRGDA1	DIV S5-S6	G1731
$hNa_v1.5$	G1743R	BRGDA1	DIV S5-S6	G1731
$hNa_v1.5$	V1764F	BRGDA1	DIV S6	V1752
$hNa_v1.5$	T1779M	BRGDA1	C-terminus	T1767
$hNa_v1.5$	E1784K	BRGDA1	C-terminus	E1772
$hNa_v1.5$	Y1795H	BRGDA1	C-terminus	Y1783
$hNa_v1.5$	Y1795YD	BRGDA1	C-terminus	Y1783
$hNa_v1.5$	Q1832E	BRGDA1	C-terminus	K1820
$hNa_v1.5$	C1850S	BRGDA1	C-terminus	C1838
$hNa_v1.5$	V1861I	BRGDA1	C-terminus	V1849
$hNa_v1.5$	K1872N	BRGDA1	C-terminus	R1860
$hNa_v1.5$	V1903L	BRGDA1	C-terminus	V1891
$hNa_v1.5$	A1924T	BRGDA1	C-terminus	I1912
$hNa_v1.5$	G1935S	BRGDA1	C-terminus	G1920
$hNa_v1.5$	E1938K	BRGDA1	C-terminus	D1923

Table 6 continued

Related proteins	Mutations	Diseases	Structural position	Map on $hNa_v1.7$
$hNa_v1.5$	V1951L	BRGDA1	C-terminus	N1936
$hNa_v1.5$	I1968S	BRGDA1	C-terminus	T1949
$hNa_v1.5$	F2004L	BRGDA1	C-terminus	D1982
$hNa_v1.5$	F2004V	BRGDA1	C-terminus	D1982
$hNa_v1.5$	T220I	SSS1	DI S4	T215
$hNa_v1.5$	A735V	SSS1	DII S1-S2	A762
$hNa_v1.5$	P1298L	SSS1	DIII S3-S4	P1285
$hNa_v1.5$	G1408R	SSS1	DIII S5-S6	G1395
$hNa_v1.5$	D1792N	SSS1	C-terminus	E1780
$hNa_v1.5$	S1710L	VF1	DIV S5-S6	S1697
$hNa_v1.5$	F532C	SIDS	DI - DII	F557
$hNa_v1.5$	S941N	SIDS	DII - DIII	S970
$hNa_v1.5$	G1084S	SIDS	DII - DIII	–
$hNa_v1.5$	S1333Y	SIDS	DIII S4-S5	S1320
$hNa_v1.5$	F1705S	SIDS	DIV S5-S6	F1692
$hNa_v1.5$	D1275N	ATRST1	DIII S3	D1262
$hNa_v1.5$	D1275N	CMD1E	DIII S3	D1262
$hNa_v1.5$	M138I	ATFB10	DI S1	M133
$hNa_v1.5$	E428K	ATFB10	DI - DII	K417
$hNa_v1.5$	H445D	ATFB10	DI - DII	Q434
$hNa_v1.5$	N470K	ATFB10	DI - DII	S472
$hNa_v1.5$	A572D	ATFB10	DI - DII	S599
$hNa_v1.5$	E655K	ATFB10	DI - DII	D682
$hNa_v1.5$	E1053K	ATFB10	DII - DIII	E1095
$hNa_v1.5$	T1131I	ATFB10	DII - DIII	E1140
$hNa_v1.5$	R1826C	ATFB10	C-terminus	L1814
$hNa_v1.5$	V1951M	ATFB10	C-terminus	N1936
$hNa_v1.5$	N1987K	ATFB10	C-terminus	E1967
$hNa_v1.5$	R222Q	MEPPC	DI S4	R217

PFHB1A: Progressive familial heart block 1A; LQT3: Long QT syndrome 3; BRGDA1: Brugada syndrome 1; SSS1: Sick sinus syndrome 1; VF1: Familial paroxysmal ventricular fibrillation 1; SIDS: Sudden infant death syndrome; ATRST1: Atrial standstill 1; CMD1E: Cardiomyopathy, dilated 1E; ATFB10: Atrial fibrillation, familial, 10; MEPPC: Multifocal ectopic Purkinje-related premature contraction.

channelopathies; and in $Na_v1.7$, $Na_v1.8$, and $Na_v1.9$ are associated with pain-related diseases (Fig. 3 and Tables 1, 2, 3, 4, 5, 6, 7, 8, 9, 10). Mapping of all Na_v channel mutations onto the $Na_v1.7$ structure model revealed that more than 80% of mutations are located in the VSDs and pore domains (Fig. 4A and 4B). Notably, disease-causing mutations are somewhat equally distributed in all four Na_v channel domains, which account for more than 20 sodium channelopathies (Fig. 4C). Furthermore, mutations are also distributed in various regions of the pore domains, suggesting that they may disturb Na_v channel functions by altering sodium ion selectivity and conductivity (Fig. 4D).

$Na_v1.2$ mutations are largely associated with various epilepsy diseases, including BFIS3 (seizures, benign familial infantile 3), EIEE11 (epileptic encephalopathy, early infantile, 11), and DS (Fig. 3B and Table 3). More than 30 $Na_v1.2$ mutations have been discovered and some of them are now functionally characterized. Interestingly, electrophysiological studies showed that $Na_v1.2$ mutations can either be loss-of-function (R1319Q and L1330F) or gain-of-function (M252V,

Table 7. Structural mapping of disease-related mutations identified in human $Na_v1.6$

Related proteins	Mutations	Diseases	Structural position	Map on $hNa_v1.7$
$hNa_v1.6$	D58N	EIEE13	N-terminus	D52
$hNa_v1.6$	F210L	EIEE13	DI S3-S4	F204
$hNa_v1.6$	G214D	EIEE13	DI S3-S4	G208
$hNa_v1.6$	N215R	EIEE13	DI S3-S4	N209
$hNa_v1.6$	V216D	EIEE13	DI S3-S4	V210
$hNa_v1.6$	R223G	EIEE13	DI S4	R217
$hNa_v1.6$	F260S	EIEE13	DI S5	F254
$hNa_v1.6$	L407F	EIEE13	DI S6	L398
$hNa_v1.6$	V410L	EIEE13	DI - DII	V401
$hNa_v1.6$	E479V	EIEE13	DI - DII	E464
$hNa_v1.6$	R530W	EIEE13	DI - DII	H515
$hNa_v1.6$	R662C	EIEE13	DI - DII	Q643
$hNa_v1.6$	T767I	EIEE13	DII S1	T758
$hNa_v1.6$	F846S	EIEE13	DII S4	F837
$hNa_v1.6$	R850Q	EIEE13	DII S4	R841
$hNa_v1.6$	L875Q	EIEE13	DII S5	L866
$hNa_v1.6$	A890T	EIEE13	DII S5	A881
$hNa_v1.6$	V960D	EIEE13	DII S6	V951
$hNa_v1.6$	N984K	EIEE13	DII - DIII	N975
$hNa_v1.6$	I1327V	EIEE13	DIII S4-S5	I1321
$hNa_v1.6$	L1331V	EIEE13	DIII S5	L1325
$hNa_v1.6$	G1451S	EIEE13	DIII S6	G1444
$hNa_v1.6$	G1451S	EIEE13	DIII S6	G1444
$hNa_v1.6$	N1466K	EIEE13	DIII S6	N1459
$hNa_v1.6$	N1466T	EIEE13	DIII S6	N1459
$hNa_v1.6$	I1479V	EIEE13	DIII - DIV	I1472
$hNa_v1.6$	E1483K	EIEE13	DIII - DIV	E1476
$hNa_v1.6$	I1583T	EIEE13	DIV S2-S3	V1576
$hNa_v1.6$	V1592L	EIEE13	DIV S3	V1585
$hNa_v1.6$	S1596C	EIEE13	DIV S3	S1589
$hNa_v1.6$	I1605R	EIEE13	DIV S3	L1598
$hNa_v1.6$	R1617Q	EIEE13	DIV S4	R1610
$hNa_v1.6$	L1621W	EIEE13	DIV S4	L1614
$hNa_v1.6$	A1650T	EIEE13	DIV S5	A1643
$hNa_v1.6$	P1719R	EIEE13	DIV S5-S6	P1713
$hNa_v1.6$	N1768D	EIEE13	DIV S6	N1762
$hNa_v1.6$	Q1801E	EIEE13	C-terminus	Q1795
$hNa_v1.6$	E1870D	EIEE13	C-terminus	E1864
$hNa_v1.6$	R1872W	EIEE13	C-terminus	R1866
$hNa_v1.6$	R1872Q	EIEE13	C-terminus	R1866
$hNa_v1.6$	R1872L	EIEE13	C-terminus	R1866
$hNa_v1.6$	N1877S	EIEE13	C-terminus	N1871

EIEE13: Epileptic encephalopathy, early infantile, 13.

Table 8. Structural mapping of disease-related mutations identified in human $Na_v1.8$

Related proteins	Mutations	Diseases	Structural position	Map on $hNa_v1.7$
$hNa_v1.8$	L554P	SFN	DI - DII	–
$hNa_v1.8$	M650K	SFN	DI - DII	Y729
$hNa_v1.8$	A1304T	SFN	DIII S5	A1344
$hNa_v1.8$	G1662S	SFN	DIV S5-S6	G1699
$hNa_v1.8$	I1706V	SFN	DIV S6	I1744

SFN: Small fiber neuropathy.

Table 9. Structural mapping of disease-related mutations identified in human $Na_v1.9$

Related proteins	Mutations	Diseases	Structural position	Map on $hNa_v1.7$
$hNa_v1.9$	R222H	FEPS3	DI S4	R214
$hNa_v1.9$	R222S	FEPS3	DI S4	R214
$hNa_v1.9$	R225C	FEPS3	DI S4	R217
$hNa_v1.9$	I381T	FEPS3	DI S6	V383
$hNa_v1.9$	G699R	FEPS3	DII S5	G864
$hNa_v1.9$	A808G	FEPS3	DII S6	A965
$hNa_v1.9$	L811P	HSAN7	DII S6	L968
$hNa_v1.9$	L1158P	FEPS3	DIII S4	L1301
$hNa_v1.9$	V1184A	HSAN7	DIII S5	V1327

FEPS3: Episodic pain syndrome, familial, 3; HSAN7: Neuropathy, hereditary sensory and autonomic, 7.

V261M, L1563V, and Y1579C) (Misra et al., 2008; Liao et al., 2010; Lauxmann et al., 2013). It is noted that BFIS3 mutations in $Na_v1.2$ create less pronounced changes in the activation and inactivation potentials than the EIEE11 mutations (Shi et al., 2012).

Only six missense mutations of $Na_v1.3$ have so far been identified in patients with cryptogenic partial epilepsy (Fig. 3C and Table 4). Five of them, namely K354Q, R357Q, D815N, E1160K, and M1372V, have been characterized, all of which are gain-of-function mutations, consistent with the neuronal hyperexcitability phenotype (Estacion et al., 2010; Vanoye et al., 2014).

$Na_v1.4$ is essential for controlling the muscle action potential and consequently crucial for skeletal muscle contraction. Mutations of $Na_v1.4$ are related with various neuromuscular disorders including PMC (paramyotonia congenita of von Eulenburg), HOKPP2 (periodic paralysis hypokalemic 2), HYPP (periodic paralysis hyperkalemic), NKPP (periodic paralysis normokalemic), MYOSCN4A (myotonia SCN4A-related), and CMS16 (myasthenic syndrome, congenital, 16) (Fig. 3D and Table 5). Different disease-causing mutations alter the $Na_v1.4$ channel function through distinct mechanisms. For example, CMS16 mutations R104H, P382T, and C1209F completely abolish the $Na_v1.4$ channel's ability to conduct sodium ion, while other mutations such as M203K, R225W, and D1069N cause reduced action potential amplitude, leading to impaired channel function (Zaharieva et al., 2016). Compared to the WT channel, a CMS16 voltage sensor mutant R1457H requires longer hyperpolarization to recover which results in increased fast inactivation (Arnold et al., 2015). On the other hand, a HOKPP2 mutation R1135H (the third arginine in the domain III voltage sensor) exhibits increased depolarization, suggesting that R1135H mutation be gain-of-function (Groome et al., 2014). A MYOSCN4A mutation I582V shows a hyperpolarizing shift of 6 mV, indicating the nature of this mutation be also gain-of-function (Corrochano et al., 2014).

$Na_v1.6$ is one of the sodium channels expressed in human brain and mutations of $Na_v1.6$ cause EIEE13 (epileptic encephalopathy, early infantile, 13) (Fig. 3F and Table 7). More than 40 $Na_v1.6$ mutations have been discovered since 2012 (Fig. 3F and Table 7), and seven of them have been studied in the functional assays. Specifically, five $Na_v1.6$ mutations, namely T767I, N984K, T1716I, N1768D, and R1872W/R1872Q/R1872L, are characterized as gain-of-function, which cause hyperpolarizing shift of inactivation voltage or increased persistent current (Veeramah et al., 2012; Estacion et al., 2014; Wagnon et al., 2016), while the

Table 10. Summary of sodium channelopathies

Related proteins	Diseases
$hNa_v1.1$	**GEFS+2**: Generalized epilepsy with febrile seizures plus 2
	EIEE6: Epileptic encephalopathy, early infantile, 6
	ICEGTC: Intractable childhood epilepsy with generalized tonic-clonic seizures
	FHM3: Migraine, familial hemiplegic, 3
	FEB3A: Febrile seizures, familial, 3A
$hNa_v1.2$	**BFIS3**: Seizures, benign familial infantile 3
	EIEE11: Epileptic encephalopathy, early infantile, 11
	DS: Dravet syndrome
$hNa_v1.3$	**CPE**: Cryptogenic partial epilepsy
$hNa_v1.4$	**PMC**: Paramyotonia congenita of von Eulenburg
	HOKPP2: Periodic paralysis hypokalemic 2
	HYPP: Periodic paralysis hyperkalemic
	NKPP: Periodic paralysis normokalemic
	MYOSCN4A: Myotonia SCN4A-related
	CMS16: Myasthenic syndrome, congenital, 16
$hNa_v1.5$	**PFHB1A**: Progressive familial heart block 1A
	LQT3: Long QT syndrome 3
	BRGDA1: Brugada syndrome 1
	SSS1: Sick sinus syndrome 1
	VF1: Familial paroxysmal ventricular fibrillation 1
	SIDS: Sudden infant death syndrome
	ATRST1: Atrial standstill 1
	CMD1E: Cardiomyopathy, dilated 1E
	ATFB10: Atrial fibrillation, familial, 10
	MEPPC: Multifocal ectopic Purkinje-related premature contraction
$hNa_v1.6$	**EIEE13**: Epileptic encephalopathy, early infantile, 13
$hNa_v1.7$	**IEM**: Primary erythermalgia
	PEPD: Paroxysmal extreme pain disorder
	CIP: Indifference to pain, congenital, autosomal recessive
	DS: Dravet syndrome
	SFN: Small fiber neuropathy
	FEB: Febrile eizures
$hNa_v1.8$	**SFN**: Small fiber neuropathy
$hNa_v1.9$	**FEPS3**: Episodic pain syndrome, familial, 3
	HSAN7: Neuropathy, hereditary sensory and autonomic, 7

other two mutations, R223G and G1451S, are loss-of-function (de Kovel et al., 2014; Blanchard et al., 2015).

Five $Na_v1.8$ mutations are associated with SFN, a condition that is clinically characterized by autonomic dysfunction and burning pain in the distal extremities (Fig. 3H and Table 8). Electrophysiology study has shown that $Na_v1.8$ mutations, specifically L554P, A1304T, G1662S, and I1706V, accelerate inactivation recovery and enhance activation, which result in hyperexcitability (Faber et al., 2012b; Huang et al., 2013; Han et al., 2014). However, another SFN $Na_v1.8$ mutation M650K causes reduced excitability of C fibers (Kist et al., 2016).

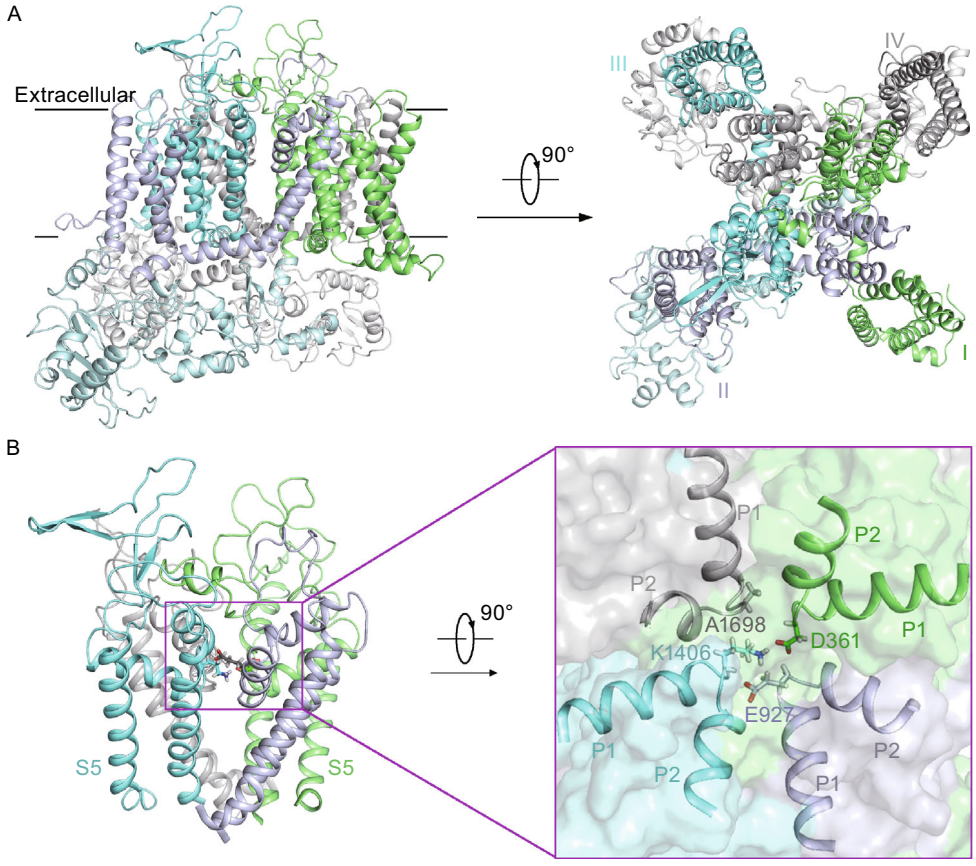

Figure 1. Homology model structure of human $Na_v1.7$ sodium channel. (A) Intra-membrane view and extracellular view of the structure model of $Na_v1.7$. The four domains are colored green, light blue, cyan, and gray for domain I, II, III, and IV, respectively. (B) The pore domain of $Na_v1.7$ structure model. The S5–S6 segments of $Na_v1.7$ are shown and the four selectivity filter amino acids are shown as sticks (left). A close-up view of the four SF residues, D361 in domain I, E927 in domain II, K1406 in domain III, and A1698 in domain IV (right).

FEPS3 (episodic pain syndrome, familial, 3) and HSAN7 (neuropathy, hereditary sensory and autonomic, 7) are thought to be caused by the nine missense gain-of-function mutations of $Na_v1.9$ (Fig. 3I and Table 9). Specifically, compared to the WT channel, R225C and A808G mutations induce hyperexcitability of the DRG neurons (Zhang et al., 2013), G699R enhances activation (Han et al., 2015), L811P significantly increases current density (Leipold et al., 2013), L1158P enhances spontaneous firing (Huang et al., 2014), and V1184A alters the channel voltage dependence that results in channel opening in response to hyperpolarized potentials (Leipold et al., 2015).

DISEASE-RELATED MUTATIONS IN SODIUM CHANNELS $NA_V1.1$ AND $NA_V1.5$

Mutations of $Na_v1.1$ are associated with several neurological disorders including GEFS+2, EIEE6, ICEGTC, FHM3 (migraine, familial hemiplegic, 3), and FEB3A (febrile seizures, familial, 3A) (Table 2 and Table 10). More than 400 mutations of $Na_v1.1$ have been identified, approximately 10% account for GEFS+2 while 80% for EIEE6 (Fig. 5A and Table 2). By mapping the $Na_v1.1$-related mutations to the $Na_v1.7$ structure model, we identified that most mutations are located in the VSDs and the pore domain (Fig. 5A). For example, mutations of the four positively charged residues, R1639G, R1642S, R1645Q, and R1648C, are present in the domain IV S4 segment (Table 2), suggesting that these EIEE6 mutations may alter the voltage sensing behavior of the channel. In addition, it is noteworthy that $Na_v1.1$ mutations can be either loss-of-function or gain-of-function (Catterall et al., 2010; Escayg and Goldin, 2010). For example, two GEFS+2 mutations W1204R and R1648H increase the level of persistent current through gain-of-function (Lossin et al., 2002), while the loss-of-function M145T mutation in FEB3A decreases 60% of the current density (Mantegazza et al., 2005).

$Na_v1.5$ is the primary sodium channel in the heart and is essential for the cardiac action potential initiation. More than 400 $Na_v1.5$ mutations have been discovered and they are

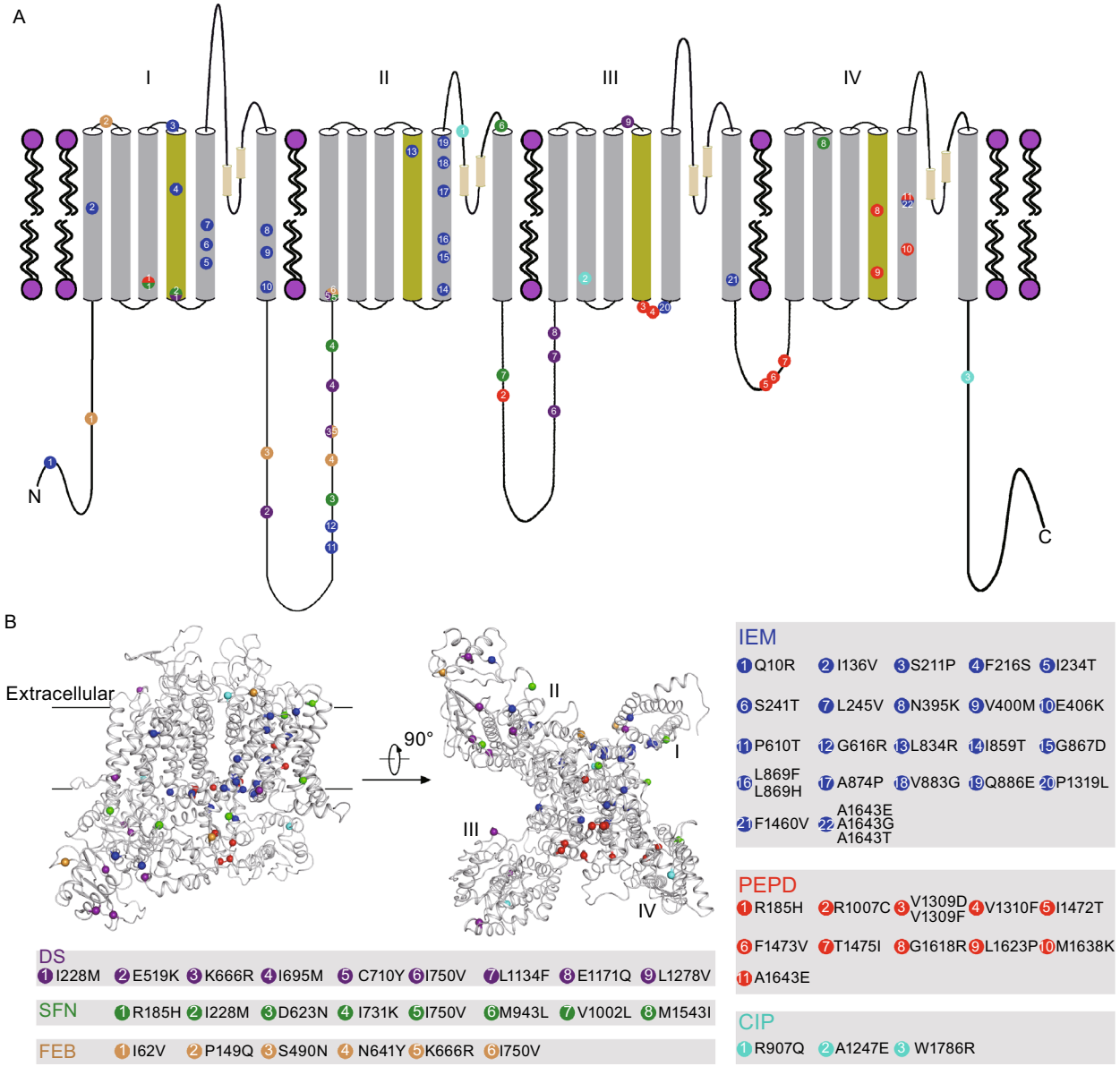

Figure 2. Amino acid locations of $Na_v1.7$ disease-related mutations on the $Na_v1.7$ structure model. (A) The topology of human $Na_v1.7$ sodium channel. Cylinders represent the transmembrane segments, which are colored in gray except that the S4 voltage-sensing segments are colored in yellow. The lines represent the soluble regions between the transmembrane segments or the N/C-terminus. The two P helices between S5 and S6 segments are shown in cylinders. Mutations of $Na_v1.7$ are discriminately mapped on the topology scheme of $Na_v1.7$ by different colors, namely, IEM (blue), PEPD (red), CIP (cyan), DS (purple), SFN (green), and FEB (pink). (B) Intra-membrane view and intracellular views of the $Na_v1.7$ structure model. Mapping of disease-related mutations onto the $Na_v1.7$ structure model is highlighted by different colors. Summary of $Na_v1.7$ mutations is shown in different gray boxes.

implicated in a wide variety of cardiac diseases—including PFHB1A (progressive familial heart block 1A), LQT3, BRGDA1, SSS1, VF1 (familial paroxysmal ventricular fibrillation 1), SIDS (sudden infant death syndrome), ATRST1 (atrial standstill 1), CMD1E (cardiomyopathy, dilated 1E), ATFB10 (atrial fibrillation, familial, 10), and MEPPC (multifocal ectopic Purkinje-related premature contractions) (Fig. 5B and Table 6). By mapping all the $Na_v1.5$ mutations onto the $Na_v1.7$ structure model, it shows that most mutations are located in the transmembrane regions of the

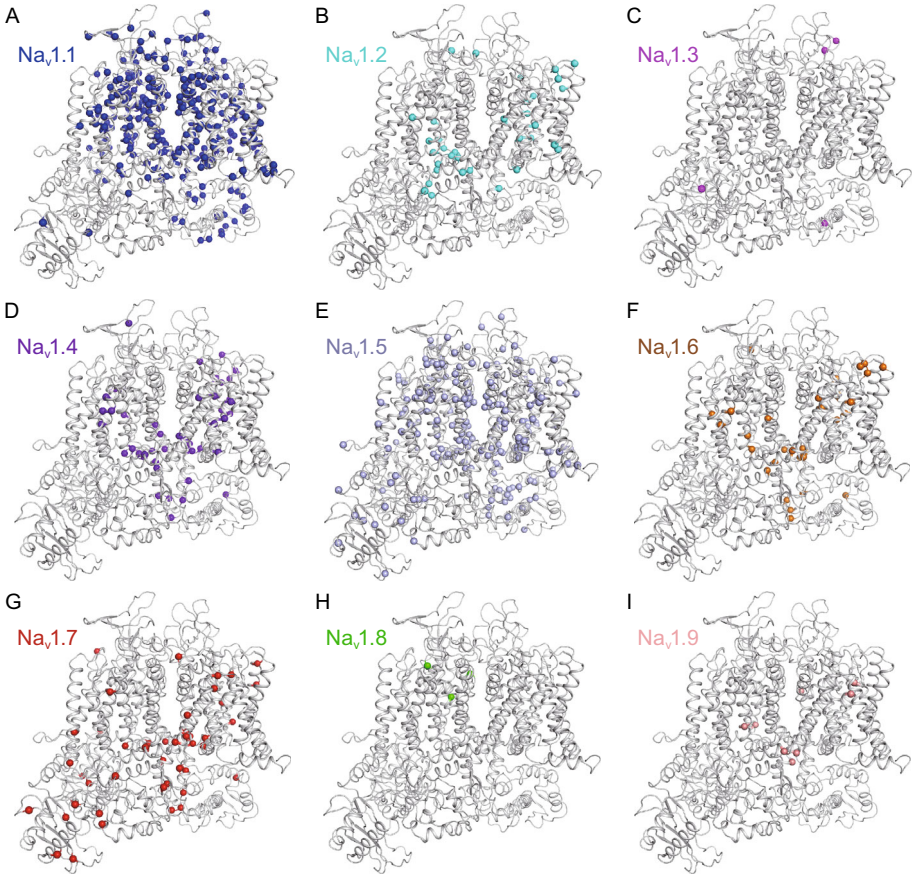

Figure 3. Mapping of Na$_v$ channel disease-related mutations onto the Na$_v$1.7 structure model. The Na$_v$1.7 channel is shown in cartoon from the intra-membrane view. The Cα atoms of the disease-related amino acids are shown in spheres. Mapped mutations from nine Na$_v$ sodium channels to the Na$_v$1.7 structure model are differentiated by distinct colors, Na$_v$1.1 (A, blue), Na$_v$1.2 (B, cyan), Na$_v$1.3 (C, magenta), Na$_v$1.4 (D, purple blue), Na$_v$1.5 (E, pale cyan), Na$_v$1.6 (F, orange), Na$_v$1.7 (G, red), Na$_v$1.8 (H, green), and Na$_v$1.9 (I, salmon).

channel, suggesting that these mutations might disturb voltage sensing or sodium conduction (Fig. 5B). Furthermore, about 50% of the Na$_v$1.5 mutations account for BRGDA1, while 30% for LQT3. Similar to the case of Na$_v$1.1, mutations in Na$_v$1.5 can be either loss-of-function or gain-of-function. For example, loss-of-function mutations are associated with BRGDA1, CMD1E, SSS1, and ATFB10 (Tan et al., 2001; Smits et al., 2005; Makiyama et al., 2008; Laurent et al., 2012), while gain-of-function mutations of Na$_v$1.5 are responsible for LQT3 (Remme et al., 2006), CMD1E, and ATFB10 (Olson et al., 2005), and most recently MEPPC (Swan et al., 2014).

CONCLUDING REMARKS

The Na$_v$ family of sodium channels are important drug targets for the pharmaceutical industry. However, no atomic structure of any mammalian Na$_v$ channels is currently available, preventing the establishment of an in-depth structure-function relationship for this important group of sodium channels and application of structure-based approach to rationally design compounds that are able to modulate the functions of those Na$_v$ channels in a disease relevant manner. Using the recently published cryo-EM structure of a rabbit Ca$_v$ channel Ca$_v$1.1, we established an atomic level heterotetrameric structure model for the human Na$_v$ channel Na$_v$1.7. Disease-related mutations of Na$_v$1.7 and other members of the Na$_v$ family, which are largely responsible for many neurological disorders like epilepsies, pains, and myopathies, are mapped onto the structure model. Taken together the available functional data, we attempted to establish a rudimentary structure-function relationship for human Na$_v$1.7 and other members of the Na$_v$ channel family. It is noticeable that sodium channelopathies can be attributed to both loss-of-function and gain-of-function mutations.

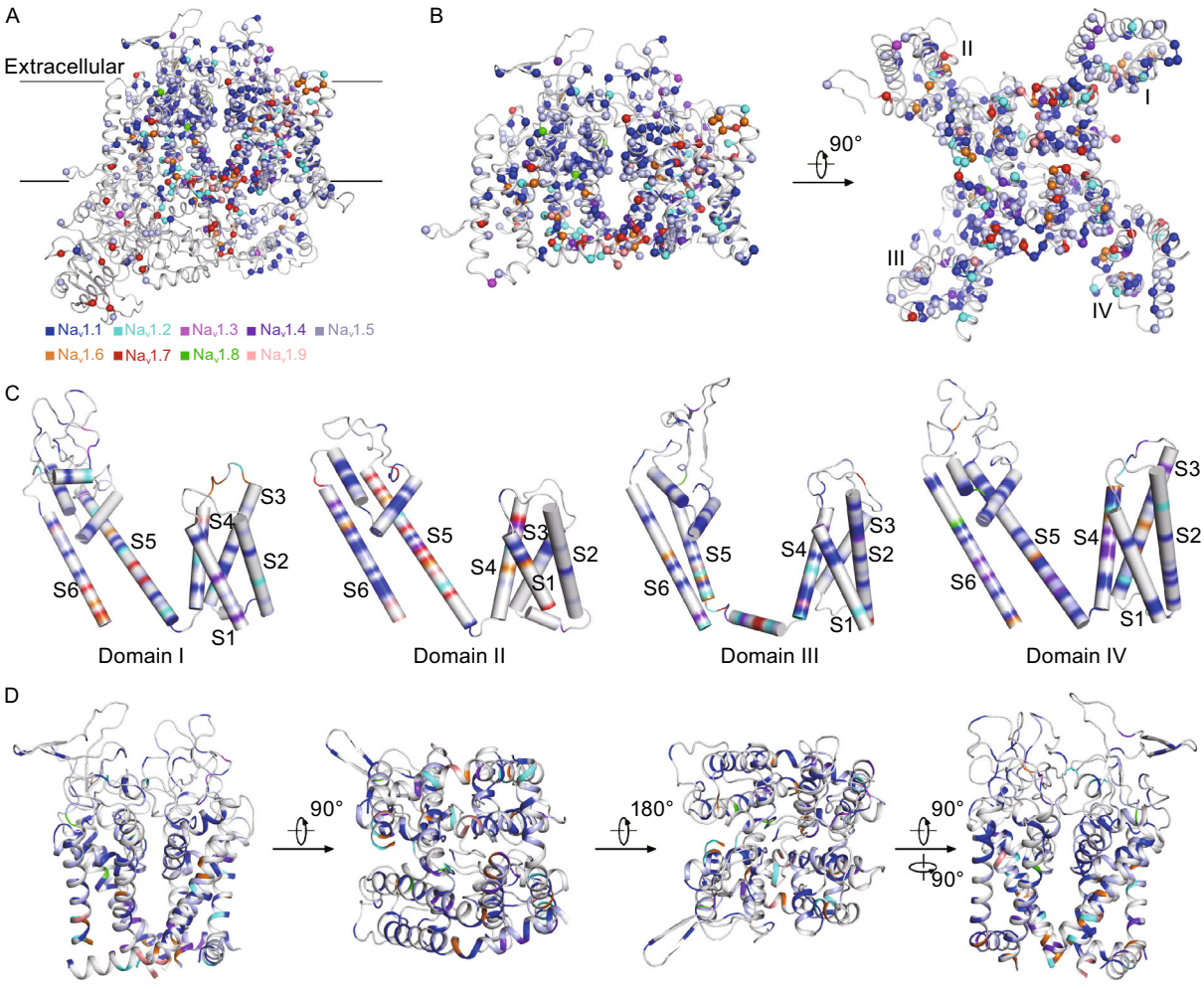

Figure 4. Mutations that cause sodium channelopathies are plotted on the $Na_v1.7$ sodium channel model. (A) The amino acid residues related with sodium channelopathies are mapped on the $Na_v1.7$ structure model. All mutated residues are shown in spheres and colored for $Na_v1.1$ (blue), $Na_v1.2$ (cyan), $Na_v1.3$ (magenta), $Na_v1.4$ (purple blue), $Na_v1.5$ (pale cyan), $Na_v1.6$ (orange), $Na_v1.7$ (red), $Na_v1.8$ (green), and $Na_v1.9$ (salmon). (B) The distribution of sodium channelopathy-related mutations on the transmembrane regions of the $Na_v1.7$ structure model. Mutations of the VSDs and the pore domain are shown from the intra-membrane and intracellular views. (C) The mutation distributions for the four domains. S1–S6 segments are shown in cylindrical helices. (D) Mapping mutations to the pore domain in four different views.

However, we must realize that the current $Na_v1.7$ structural model has its limitation and the atomic resolution mammalian Na_v channel structure is urgently needed. In recent years, cryo-EM technology is becoming a mainstream technology for structural biology, which is able to potentially overcome the significant technical hurdles in producing challenging proteins such as mammalian Na_v channels in sufficient quality and the necessity of crystallization for structural elucidation. Detailed mechanisms of how the Na_v channels sense voltage changes and conduct sodium ions can only be answered when such atomic resolution structures become available. We hope the $Na_v1.7$ structure model presented here is a temporary surrogate to help understand the Na_v channel functions, particularly those relevant to the various neurological diseases, at atomic level, and contributes to the structure-based rational design of the next generation Na_v channel modulators.

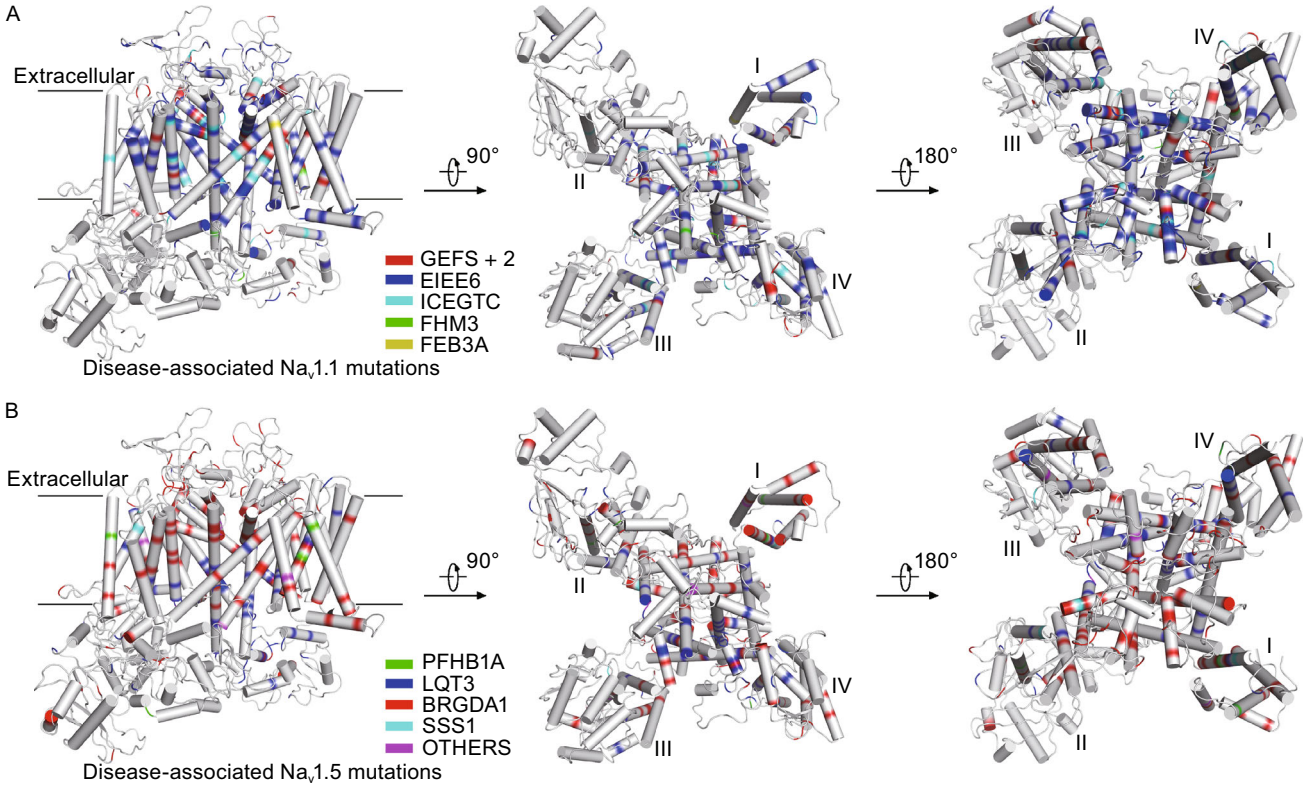

Figure 5. Distributions of the missense mutations in Na$_v$1.1 and Na$_v$1.5. (A) Distributions of Na$_v$1.1 missense mutations on the Na$_v$1.7 model structure. More than 400 mutations are mapped. Mutations from five Na$_v$1.1-related diseases are shown from intra-membrane, intracellular, and extracellular views. The Na$_v$1.7 model is shown in cylindrical helices and colored by GEFS+2 in red, EIEE6 in blue, ICEGTC in cyan, FHM3 in green, and FEB3A in yellow. (B) Distributions of Na$_v$1.5 related-disease mutations on the Na$_v$1.7 structure model. Mutations from Na$_v$1.5 related diseases are shown from intra-membrane, intracellular, and extracellular views. Different diseases are colored in green for PFHB1A, blue for LQT3, red for BRGDA1, cyan for SSS1, and magenta for VF1, SIDS, ATRST1, CMD1E, ATFB10, and MEPPC.

SUMMARY OF DISEASE-RELATED MUTATIONS FOR SODIUM CHANNELS

Most of the Na$_v$ channel disease-related mutations are extracted from the UNIPROT websites:

http://www.uniprot.org/uniprot/P35498 (Na$_v$1.1);
http://www.uniprot.org/uniprot/Q99250 (Na$_v$1.2);
http://www.uniprot.org/uniprot/P35499 (Na$_v$1.4);
http://www.uniprot.org/uniprot/Q14524 (Na$_v$1.5);
http://www.uniprot.org/uniprot/Q9UQD0 (Na$_v$1.6);
http://www.uniprot.org/uniprot/Q15858 (Na$_v$1.7);
http://www.uniprot.org/uniprot/Q9Y5Y9 (Na$_v$1.8);
http://www.uniprot.org/uniprot/Q9UI33 (Na$_v$1.9).

In the UNIPROT websites, there are no mutations described for Na$_v$1.3. During literatures searching, we found that six mutations of Na$_v$1.3 are associated with cryptogenic partial epilepsy. Except for the present mutations in the UNIPROT websites, we found additional mutations of Na$_v$ channels in literatures. All mutations are summarized in Tables 1, 2, 3, 4, 5, 6, 7, 8, 9. However, we recognize that our summary may not contain all Na$_v$ channel disease-related mutations owing to abundant literatures reporting Na$_v$ channel disease-related mutations and increasing volume of work describing new findings.

ACKNOWLEDGEMENTS

This work was supported by funds from the National Basic Research Program (973 Program) (2015CB910101, 2016YFA0500402, 2014ZX09507003-006), the National Natural Science Foundation of China (projects 31621092, 31630017, and 31611130036). The research of N.Y. was supported in part by an International Early Career Scientist grant from the Howard Hughes Medical Institute and an endowed professorship from Bayer Healthcare.

ABBREVIATIONS

ATRST1, atrial standstill 1; BRGDA1, Brugada syndrome 1; Ca$_v$, voltage-gated calcium; CNS, central nervous system; cryo-EM, cryo-electron microscopy; DS, Dravet syndrome; FEB, febrile seizure; GEFS+2, generalized epilepsy with febrile seizures plus 2; HOKPP2, periodic paralysis hypokalemic 2; HYPP, periodic paralysis hyperkalemic; IEM, primary erythermalgia; LQT3, long QT

syndrome 3; MEPPC, multifocal ectopic Purkinje-related premature contractions; Na_v, voltage-gated sodium; NKPP, periodic paralysis normokalemic; PEPD, paroxysmal extreme pain disorder; PFHB1A, progressive familial heart block 1A; PMC, paramyotonia congenita of von Eulenburg; SF, selectivity filter; SFN, small fiber neuropathy; SIDS, sudden infant death syndrome; SSS1, sick sinus syndrome 1; VF1, familial paroxysmal ventricular fibrillation 1; VSDs, voltage-sensing domains

COMPLIANCE WITH ETHICS GUIDELINES

Weiyun Huang, Minhao Liu, S. Frank Yan, and Nieng Yan declare that they have no conflict of interest. This article does not contain any studies with human or animal subjects performed by any of the authors.

OPEN ACCESS

REFERENCES

Arnold WD, Feldman DH, Ramirez S, He L, Kassar D, Quick A, Klassen TL, Lara M, Nguyen J, Kissel JT et al (2015) Defective fast inactivation recovery of Nav 1.4 in congenital myasthenic syndrome. Ann Neurol 77:840–850

Blanchard MG, Willemsen MH, Walker JB, Dib-Hajj SD, Waxman SG, Jongmans MC, Kleefstra T, van de Warrenburg BP, Praamstra P, Nicolai J et al (2015) De novo gain-of-function and loss-of-function mutations of SCN8A in patients with intellectual disabilities and epilepsy. J Med Genet 52:330–337

Catterall WA (2000) From ionic currents to molecular mechanisms: the structure and function of voltage-gated sodium channels. Neuron 26:13–25

Catterall WA (2012a) Sodium channel mutations and epilepsy. In: Noebels JL, Avoli M, Rogawski MA, Olsen RW, Delgado-Escueta AV (eds) Jasper's basic mechanisms of the epilepsies. National Center for Biotechnology Information (US), Bethesda

Catterall WA (2012b) Voltage-gated sodium channels at 60: structure, function and pathophysiology. J Physiol 590:2577–2589

Catterall WA (2014) Structure and function of voltage-gated sodium channels at atomic resolution. Exp Physiol 99:35–51

Catterall WA, Goldin AL, Waxman SG (2005) International Union of Pharmacology. XLVII. Nomenclature and structure-function relationships of voltage-gated sodium channels. Pharmacol Rev 57:397–409

Catterall WA, Kalume F, Oakley JC (2010) NaV1.1 channels and epilepsy. J Physiol 588:1849–1859

Choi JS, Dib-Hajj SD, Waxman SG (2006) Inherited erythermalgia: limb pain from an S4 charge-neutral Na channelopathy. Neurology 67:1563–1567

Choi JS, Zhang L, Dib-Hajj SD, Han C, Tyrrell L, Lin Z, Wang X, Yang Y, Waxman SG (2009) Mexiletine-responsive erythromelalgia due to a new Na(v)1.7 mutation showing use-dependent current fall-off. Exp Neurol 216:383–389

Choi JS, Boralevi F, Brissaud O, Sanchez-Martin J, Te Morsche RH, Dib-Hajj SD, Drenth JP, Waxman SG (2011) Paroxysmal extreme pain disorder: a molecular lesion of peripheral neurons. Nat Rev Neurol 7:51–55

Corrochano S, Mannikko R, Joyce PI, McGoldrick P, Wettstein J, Lassi G, Raja Rayan DL, Blanco G, Quinn C, Liavas A et al (2014) Novel mutations in human and mouse SCN4A implicate AMPK in myotonia and periodic paralysis. Brain 137:3171–3185

Corry B, Thomas M (2012) Mechanism of ion permeation and selectivity in a voltage gated sodium channel. J Am Chem Soc 134:1840–1846

de Kovel CG, Meisler MH, Brilstra EH, van Berkestijn FM, van't Slot R, van Lieshout S, Nijman IJ, O'Brien JE, Hammer MF, Estacion M et al (2014) Characterization of a de novo SCN8A mutation in a patient with epileptic encephalopathy. Epilepsy Res 108:1511–1518

Dib-Hajj SD, Estacion M, Jarecki BW, Tyrrell L, Fischer TZ, Lawden M, Cummins TR, Waxman SG (2008) Paroxysmal extreme pain disorder M1627K mutation in human $Na_v1.7$ renders DRG neurons hyperexcitable. Mol Pain 4:37

Dib-Hajj SD, Yang Y, Black JA, Waxman SG (2013) The Na(V)1.7 sodium channel: from molecule to man. Nat Rev Neurosci 14:49–62

Djouhri L, Newton R, Levinson SR, Berry CM, Carruthers B, Lawson SN (2003) Sensory and electrophysiological properties of guinea-pig sensory neurones expressing Nav 1.7 (PN1) Na+ channel alpha subunit protein. J Physiol 546:565–576

Escayg A, Goldin AL (2010) Sodium channel SCN1A and epilepsy: mutations and mechanisms. Epilepsia 51:1650–1658

Estacion M, Dib-Hajj SD, Benke PJ, Te Morsche RH, Eastman EM, Macala LJ, Drenth JP, Waxman SG (2008) NaV1.7 gain-of-function mutations as a continuum: A1632E displays physiological changes associated with erythromelalgia and paroxysmal extreme pain disorder mutations and produces symptoms of both disorders. J Neurosci 28:11079–11088

Estacion M, Gasser A, Dib-Hajj SD, Waxman SG (2010) A sodium channel mutation linked to epilepsy increases ramp and persistent current of Nav1.3 and induces hyperexcitability in hippocampal neurons. Exp Neurol 224:362–368

Estacion M, O'Brien JE, Conravey A, Hammer MF, Waxman SG, Dib-Hajj SD, Meisler MH (2014) A novel de novo mutation of SCN8A (Nav1.6) with enhanced channel activation in a child with epileptic encephalopathy. Neurobiol Dis 69:117–123

Faber CG, Hoeijmakers JG, Ahn HS, Cheng X, Han C, Choi JS, Estacion M, Lauria G, Vanhoutte EK, Gerrits MM et al (2012a) Gain of function Nanu1.7 mutations in idiopathic small fiber neuropathy. Ann Neurol 71:26–39

Faber CG, Lauria G, Merkies IS, Cheng X, Han C, Ahn HS, Persson AK, Hoeijmakers JG, Gerrits MM, Pierro T et al (2012b) Gain-of-function Nav1.8 mutations in painful neuropathy. Proc Natl Acad Sci USA 109:19444–19449

Fertleman CR, Baker MD, Parker KA, Moffatt S, Elmslie FV, Abrahamsen B, Ostman J, Klugbauer N, Wood JN, Gardiner

RM et al (2006) SCN9A mutations in paroxysmal extreme pain disorder: allelic variants underlie distinct channel defects and phenotypes. Neuron 52:767–774

George AL Jr (2005) Inherited disorders of voltage-gated sodium channels. J Clin Invest 115:1990–1999

Goldin AL (2001) Resurgence of sodium channel research. Annu Rev Physiol 63:871–894

Groome JR, Lehmann-Horn F, Fan C, Wolf M, Winston V, Merlini L, Jurkat-Rott K (2014) NaV1.4 mutations cause hypokalaemic periodic paralysis by disrupting IIIS4 movement during recovery. Brain 137:998–1008

Han C, Vasylyev D, Macala LJ, Gerrits MM, Hoeijmakers JG, Bekelaar KJ, Dib-Hajj SD, Faber CG, Merkies IS, Waxman SG (2014) The G1662S NaV1.8 mutation in small fibre neuropathy: impaired inactivation underlying DRG neuron hyperexcitability. J Neurol Neurosurg Psychiatry 85:499–505

Han C, Yang Y, de Greef BT, Hoeijmakers JG, Gerrits MM, Verhamme C, Qu J, Lauria G, Merkies IS, Faber CG et al (2015) The domain II S4-S5 linker in Nav1.9: a missense mutation enhances activation, impairs fast inactivation, and produces human painful neuropathy. Neuromol Med 17:158–169

Heinemann SH, Terlau H, Stuhmer W, Imoto K, Numa S (1992) Calcium channel characteristics conferred on the sodium channel by single mutations. Nature 356:441–443

Huang J, Yang Y, Zhao P, Gerrits MM, Hoeijmakers JG, Bekelaar K, Merkies IS, Faber CG, Dib-Hajj SD, Waxman SG (2013) Small-fiber neuropathy Nav1.8 mutation shifts activation to hyperpolarized potentials and increases excitability of dorsal root ganglion neurons. J Neurosci 33:14087–14097

Huang J, Han C, Estacion M, Vasylyev D, Hoeijmakers JG, Gerrits MM, Tyrrell L, Lauria G, Faber CG, Dib-Hajj SD et al (2014) Gain-of-function mutations in sodium channel Na(v)1.9 in painful neuropathy. Brain 137:1627–1642

Jarecki BW, Sheets PL, Jackson JO 2nd, Cummins TR (2008) Paroxysmal extreme pain disorder mutations within the D3/S4-S5 linker of Nav1.7 cause moderate destabilization of fast inactivation. J Physiol 586:4137–4153

Kim JB (2014) Channelopathies. Korean J Pediatr 57:1–18

Kist AM, Sagafos D, Rush AM, Neacsu C, Eberhardt E, Schmidt R, Lunden LK, Orstavik K, Kaluza L, Meents J et al (2016) SCN10A mutation in a patient with erythromelalgia enhances C-fiber activity dependent slowing. PLoS One 11:e0161789

Lampert A, Dib-Hajj SD, Tyrrell L, Waxman SG (2006) Size matters: erythromelalgia mutation S241T in Nav1.7 alters channel gating. J Biol Chem 281:36029–36035

Lampert A, O'Reilly AO, Reeh P, Leffler A (2010) Sodium channelopathies and pain. Pflugers Arch 460:249–263

Laurent G, Saal S, Amarouch MY, Beziau DM, Marsman RF, Faivre L, Barc J, Dina C, Bertaux G, Barthez O et al (2012) Multifocal ectopic Purkinje-related premature contractions: a new SCN5A-related cardiac channelopathy. J Am Coll Cardiol 60:144–156

Lauxmann S, Boutry-Kryza N, Rivier C, Mueller S, Hedrich UB, Maljevic S, Szepetowski P, Lerche H, Lesca G (2013) An SCN2A mutation in a family with infantile seizures from Madagascar reveals an increased subthreshold Na(+) current. Epilepsia 54:e117–e121

Leipold E, Liebmann L, Korenke GC, Heinrich T, Giesselmann S, Baets J, Ebbinghaus M, Goral RO, Stodberg T, Hennings JC et al (2013) A de novo gain-of-function mutation in SCN11A causes loss of pain perception. Nat Genet 45:1399–1404

Leipold E, Hanson-Kahn A, Frick M, Gong P, Bernstein JA, Voigt M, Katona I, OliverGoral R, Altmuller J, Nurnberg P et al (2015) Cold-aggravated pain in humans caused by a hyperactive NaV1.9 channel mutant. Nat Commun 6:10049

Liao Y, Deprez L, Maljevic S, Pitsch J, Claes L, Hristova D, Jordanova A, Ala-Mello S, Bellan-Koch A, Blazevic D et al (2010) Molecular correlates of age-dependent seizures in an inherited neonatal-infantile epilepsy. Brain 133:1403–1414

Lossin C, Wang DW, Rhodes TH, Vanoye CG, George AL Jr (2002) Molecular basis of an inherited epilepsy. Neuron 34:877–884

Makiyama T, Akao M, Shizuta S, Doi T, Nishiyama K, Oka Y, Ohno S, Nishio Y, Tsuji K, Itoh H et al (2008) A novel SCN5A gain-of-function mutation M1875T associated with familial atrial fibrillation. J Am Coll Cardiol 52:1326–1334

Mantegazza M, Gambardella A, Rusconi R, Schiavon E, Annesi F, Cassulini RR, Labate A, Carrideo S, Chifari R, Canevini MP et al (2005) Identification of an Nav1.1 sodium channel (SCN1A) loss-of-function mutation associated with familial simple febrile seizures. Proc Natl Acad Sci USA 102:18177–18182

Misra SN, Kahlig KM, George AL Jr (2008) Impaired NaV1.2 function and reduced cell surface expression in benign familial neonatal-infantile seizures. Epilepsia 49:1535–1545

MOE (2016) Molecular operating environment (MOE), 2013.08. Chemical Computing Group Inc, Montreal

Olson TM, Michels VV, Ballew JD, Reyna SP, Karst ML, Herron KJ, Horton SC, Rodeheffer RJ, Anderson JL (2005) Sodium channel mutations and susceptibility to heart failure and atrial fibrillation. JAMA 293:447–454

Payandeh J, Scheuer T, Zheng N, Catterall WA (2011) The crystal structure of a voltage-gated sodium channel. Nature 475:353–358

Plummer NW, Meisler MH (1999) Evolution and diversity of mammalian sodium channel genes. Genomics 57:323–331

Remme CA, Verkerk AO, Nuyens D, van Ginneken AC, van Brunschot S, Belterman CN, Wilders R, van Roon MA, Tan HL, Wilde AA et al (2006) Overlap syndrome of cardiac sodium channel disease in mice carrying the equivalent mutation of human SCN5A-1795insD. Circulation 114:2584–2594

Shi X, Yasumoto S, Kurahashi H, Nakagawa E, Fukasawa T, Uchiya S, Hirose S (2012) Clinical spectrum of SCN2A mutations. Brain Dev 34:541–545

Smits JP, Koopmann TT, Wilders R, Veldkamp MW, Opthof T, Bhuiyan ZA, Mannens MM, Balser JR, Tan HL, Bezzina CR et al (2005) A mutation in the human cardiac sodium channel (E161K) contributes to sick sinus syndrome, conduction disease and Brugada syndrome in two families. J Mol Cell Cardiol 38:969–981

Song W, Shou W (2012) Cardiac sodium channel Nav1.5 mutations and cardiac arrhythmia. Pediatr Cardiol 33:943–949

Sun YM, Favre I, Schild L, Moczydlowski E (1997) On the structural basis for size-selective permeation of organic cations through the voltage-gated sodium channel—effect of alanine mutations at the DEKA locus on selectivity, inhibition by Ca2+ and H+, and molecular sieving. J Gen Physiol 110:693–715

Suter MR, Bhuiyan ZA, Laedermann CJ, Kuntzer T, Schaller M, Stauffacher MW, Roulet E, Abriel H, Decosterd I, Wider C (2015)

p. L1612P, a novel voltage-gated sodium channel Nav1.7 mutation inducing a cold sensitive paroxysmal extreme pain disorder. Anesthesiology 122:414–423

Swan H, Amarouch MY, Leinonen J, Marjamaa A, Kucera JP, Laitinen-Forsblom PJ, Lahtinen AM, Palotie A, Kontula K, Toivonen L et al (2014) Gain-of-function mutation of the SCN5A gene causes exercise-induced polymorphic ventricular arrhythmias. Circ Cardiovasc Genet 7:771–781

Tan HL, Bink-Boelkens MT, Bezzina CR, Viswanathan PC, Beaufort-Krol GC, van Tintelen PJ, van den Berg MP, Wilde AA, Balser JR (2001) A sodium-channel mutation causes isolated cardiac conduction disease. Nature 409:1043–1047

Tikhonov DB, Zhorov BS (2012) Architecture and pore block of eukaryotic voltage-gated sodium channels in view of NavAb bacterial sodium channel structure. Mol Pharmacol 82:97–104

Vanoye CG, Gurnett CA, Holland KD, George AL Jr, Kearney JA (2014) Novel SCN3A variants associated with focal epilepsy in children. Neurobiol Dis 62:313–322

Vassilev PM, Scheuer T, Catterall WA (1988) Identification of an intracellular peptide segment involved in sodium channel inactivation. Science 241:1658–1661

Veeramah KR, O'Brien JE, Meisler MH, Cheng X, Dib-Hajj SD, Waxman SG, Talwar D, Girirajan S, Eichler EE, Restifo LL et al (2012) De novo pathogenic SCN8A mutation identified by whole-genome sequencing of a family quartet affected by infantile epileptic encephalopathy and SUDEP. Am J Hum Genet 90:502–510

Veerman CC, Wilde AA, Lodder EM (2015) The cardiac sodium channel gene SCN5A and its gene product NaV1.5: role in physiology and pathophysiology. Gene 573:177–187

Wagnon JL, Barker BS, Hounshell JA, Haaxma CA, Shealy A, Moss T, Parikh S, Messer RD, Patel MK, Meisler MH (2016) Pathogenic mechanism of recurrent mutations of SCN8A in epileptic encephalopathy. Ann Clin Transl Neurol 3:114–123

West JW, Patton DE, Scheuer T, Wang Y, Goldin AL, Catterall WA (1992) A cluster of hydrophobic amino acid residues required for fast Na(+)-channel inactivation. Proc Natl Acad Sci USA 89:10910–10914

Wu J, Yan Z, Li Z, Yan C, Lu S, Dong M, Yan N (2015) Structure of the voltage-gated calcium channel Cav1.1 complex. Science 350:aad2395

Wu J, Yan Z, Li Z, Qian X, Lu S, Dong M, Zhou Q, Yan N (2016) Structure of the voltage-gated calcium channel Cav1.1 at 3.6 A resolution. Nature 537:191–196

Yang Y, Dib-Hajj SD, Zhang J, Zhang Y, Tyrrell L, Estacion M, Waxman SG (2012) Structural modelling and mutant cycle analysis predict pharmacoresponsiveness of a Na(V)1.7 mutant channel. Nat Commun 3:1186

Yang Y, Huang J, Mis MA, Estacion M, Macala L, Shah P, Schulman BR, Horton DB, Dib-Hajj SD, Waxman SG (2016) Nav 1.7-A1632G mutation from a family with inherited erythromelalgia: enhanced firing of dorsal root ganglia neurons evoked by thermal stimuli. J Neurosci 36:7511–7522

Zaharieva IT, Thor MG, Oates EC, van Karnebeek C, Hendson G, Blom E, Witting N, Rasmussen M, Gabbett MT, Ravenscroft G et al (2016) Loss-of-function mutations in SCN4A cause severe foetal hypokinesia or 'classical' congenital myopathy. Brain 139:674–691

Zhang X, Ren W, DeCaen P, Yan C, Tao X, Tang L, Wang J, Hasegawa K, Kumasaka T, He J et al (2012) Crystal structure of an orthologue of the NaChBac voltage-gated sodium channel. Nature 486:130–134

Zhang XY, Wen J, Yang W, Wang C, Gao L, Zheng LH, Wang T, Ran K, Li Y, Li X et al (2013) Gain-of-function mutations in SCN11A cause familial episodic pain. Am J Hum Genet 93:957–966